

EXTRACTION III - FAST RESONANT EXTRACTION

M. Harrison

February 27, 1979

Summary

In this report we shall investigate the properties of the fast extraction system briefly outlined in UPC No. 27. We demonstrate the stability of the extracted beam with respect to the size of the circulating beam, and then consider the stabilization of the extracted beam, using local bump magnets, throughout the fast extraction cycle. We conclude with an estimate of the time dependence of the extracted beam for various pulsed quadrupole field strengths.

In the second Tevatron design report on extraction (UPC No. 27) we demonstrated how a system of conventional pulsed quadrupoles located in the mini-straight sections together with quadrupoles and octopoles of the correction coil package gave an average fast extraction phase space trajectory which remained essentially constant for different values of the pulsed quadrupole field gradient. We shall now define this phase space trajectory more rigorously and look at how the trajectories of individual particles relate to this average trajectory.

The equations of motion governing a one-half integer particle trajectory in normalized phase space ($y = \beta x' + \alpha x$) to the lowest order are given by

$$\frac{dx}{dn} = -2\delta y \quad (1)$$

$$\frac{dy}{dn} = -\Delta x, \quad (2)$$

where $\delta = 2\pi (\frac{1}{2} - \nu)$

ν = fractional machine tune

$\Delta = 2A - \delta$

A = quadrupole field strength
defined by $\beta\theta = Ax$

and n = number of turns.

In order to keep the mathematics simple we have omitted the terms in (1) and (2) generated by the extraction octopoles. This approximation is a good one for the types of extraction systems that we have been considering, where the particle trajectories are dominated by the quadrupole terms. This fact can be verified by noting that the separatrix trajectories (Fig. 1) be more-or-less on a straight line with the step size increasing linearly with position (quadrupole-type behavior) rather than an arc with the step size varying as the cube of position (octopole-type behavior). From (1) and (2) we get:

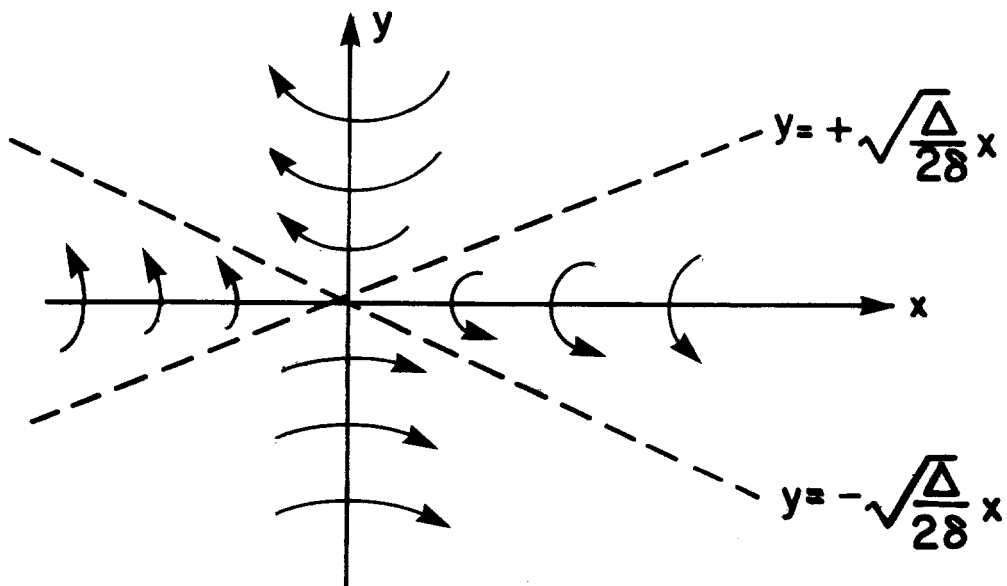
$$\frac{dy}{dx} = \frac{\Delta}{2\delta} \frac{x}{y}$$

$$\rightarrow y^2 = \frac{\Delta}{2\delta} x^2 + C \text{ (the equation of a hyperbola)}$$

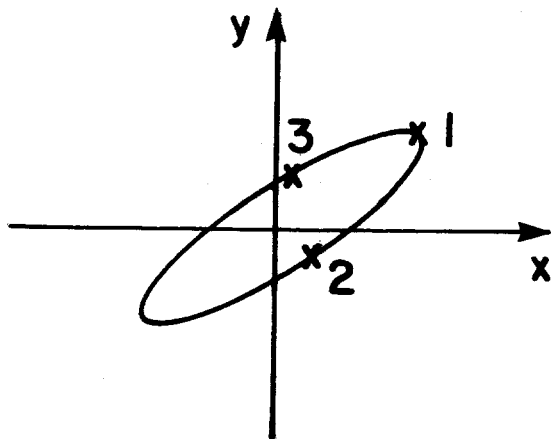
using the initial conditions that $y_0 = x_0 = 0$ then $C = 0$ and

$$y^2 = \frac{\Delta}{2\delta} x^2,$$

noting also that dx/dn (dy/dn) changes sign at $y(x) = 0$ then the individual particle trajectories will look like the drawing at the top of the next page



where the individual trajectories approach the average trajectory [$y = \pm (\Delta/2\delta)^{\frac{1}{2}} x$] asymptotically. We shall now demonstrate that provided the offset of the electrostatic septum is > 10 mms then the particle trajectories have essentially reached this average trajectory before encountering the septum. The way we have chosen to do this is to pick some extreme points in the stable phase space ellipse (0.05π mm-mrad):



and look at the individual trajectories. Figures 2, 3, and 4 show expanded views of the start of the trajectories indicated above. Figure 4 clearly demonstrates the hyperbolic behavior of the trajectories. Figures 5, 6,

and 7 show the full trajectories out to the electrostatic septum (14 mms offset) from these plots one can see that the trajectories originating at different points of the phase space ellipse and essentially colinear for amplitudes greater than 100 mms. We therefore conclude that the finite beam size will not cause any enlargement of the extracted beam phase space.

Now that we have demonstrated the stability of the fast extracted beam with respect to an average phase space trajectory we shall use this average trajectory to investigate extraction efficiency and step size during the fast spill.

We noted in UPC No. 27 that as the fast quadrupole field strength increases then the step size across the septum also increases if everything else stays constant. For the maximum field gradient we are considering (120 g/cm, 84 in. magnet) then the step size has increased from 10 mms to 20 mms, well outside of the design aperture of the extraction channel. Stabilization of the step size is accomplished by using the bump magnets to move the circulating beam closer to the septum during the fast extraction cycle. In fact by applying a similarly shaped pulse to both the bump magnets and the quadrupoles then a dynamic stabilization is possible throughout the cycle. Pulsing the bump magnets with 2 - 3 ms wide half sine wave pulses of the required strength (\leq 50 A) is difficult (though not impossible) to accomplish and in view of this fact we shall also look at the case where the local orbit perturbation (i.e., septum offset) stays constant throughout the cycle.

Figures 8, 9, and 10 show the behavior of the fast extraction phase space trajectory at the electrostatic septum for 3 values of the quadrupole field strength with the septum offset fixed at 14 mms. As noted in UPC No. 27, for the maximum field gradient, the step size has increased from 10 mms to 20 mms. Figure 11 shows a similar trajectory to that given in Fig. 10 but with the septum offset reduced to 8 mms. With this reduced septum offset then the step size has been brought back into line with the design value of 10 mms. The effect of using the bump magnets to reduce the effective septum offset is demonstrated in Fig. 12 where we use a 14 mm offset and a 6 mm local bump to create an effective 8 mm septum offset. As one can now see the fast extraction trajectory is now starting to lie very close to the slow extraction trajectory (Fig. 1). The values of the spatial and angular orbit bumps (Pos and Ang) needed to correct this trajectory are given on the plot. Figures 13 and 14 show the adjusted trajectories for the smaller quadrupole field strengths. The reasonably good correspondence between the values of Pos and Ang and the quadrupole field strength shows how an identical excitation of the bump magnets and the fast extraction quadrupoles does indeed apply a dynamic stability to the extracted beam.

In order to estimate how the extraction efficiency varies during the extraction cycle, we have used Eq. (29) from UPC No. 34 with the simplifying assumption that the step size is quadrupole dominated which gives

$$\epsilon = \frac{4W}{(x_s + \Delta)} \left[\frac{1}{2f \log_e^{1/f^2}} \right]$$

where ϵ → extraction inefficiency

W → septum width (0.075 mm)

x_s → septum offset

Δ → step size from septum

$$f \rightarrow \left(\frac{x_s}{x_s + \Delta} \right)$$

which gives

Quad Field Strength	x_s mm	Δ mm	ϵ %
-	14	10	0.99
40 g/cm	13	10	1.01
80 g/cm	11	10	1.05
120 g/cm	8	10	1.23

and hence we have an average increase in extraction losses of ~ 10-20%.

In order to determine how the extracted beam phase space will look we have taken the slow extraction trajectory from Fig. 1 and superimposed the trajectories of Figs. 12 through 14 (the solid lines), the results of which are shown in Fig. 15. The stability of the trajectories is readily apparent.

If we are unable to pulse the bump magnets as fast as the extraction quadrupoles then we would have a situation where the bump magnets would effectively have a constant value throughout the fast spill. The magnitude of this bump magnet setting is determined by the requirement of keeping maximum step size within the extraction aperture of 10 mms which for our

case is 6.0 mms in position and 15 mrad in angle (Fig. 12). Figures 16 and 17 show the trajectories for the lower quadrupole strengths with Pos and Ang fixed. From these results we can calculate the extraction efficiencies in a similar fashion to before:

Quad Field Strength	x_s mm	Δ mm	$\epsilon \%$
40 g/cm	8	4.5	2.1
80 g/cm	8	6.5	1.58
120 g/cm	8	10.0	1.23

The reduced step size for the lower field strengths causes a large rise in extraction losses, up ~ 90% from the slow extraction values.

One of the design criteria for the fast extraction system which we have not so far considered is the time dependence of the extracted beam. The design goal is to be able to extract all the circulating beam in ~ 1 ms which corresponds to some 50 turns in the machine.

Differentiating Eq. (1) with respect to n we get

$$\frac{d^2x}{dn^2} = -2\delta \frac{dy}{dn} = 2\delta \Delta x$$

put $f = 2\delta \Delta$ then

$$\frac{d^2x}{dn^2} = fx$$

$$\Leftrightarrow x = Ae^{\sqrt{f}n} + Be^{-\sqrt{f}n} \quad (3)$$

and $y = \frac{\sqrt{f}}{2\delta} \left(Ae^{\sqrt{f}n} - Be^{-\sqrt{f}n} \right)$. (4)

Taking the initial conditions $n = 0$, $x = x_0$, $y = y_0$ and solving for A and B, we get

$$A = \frac{x_0}{2} - \frac{d}{\sqrt{f}} y_0 \quad (5)$$

$$B = \frac{x_0}{2} + \frac{d}{\sqrt{f}} y_0 \quad (6)$$

for a given particle in phase space (i.e., a given x_0 , y_0) we can use Eqs. (3) and (4) to calculate how many turns that particle will take before it reaches the septum. Using the computer we can obviously do the same thing. A finite phase space area however presents a potential infinite number of initial conditions. We are therefore left with a problem of which ones to choose. Looking at Eqs. (5) and (6) we have that as x_0 , $y_0 \rightarrow 0$, then A and $B \rightarrow 0$ and $n \rightarrow \infty$. Besides this effect, particles originating close to the ingoing separatrix will initially move towards the stable phase space region rather than away from it. To obtain our initial conditions for these calculations we have taken an ellipse of the same aspect ratio as the stable phase space ellipse encompassing only the central 2% of the phase space area and picked initial conditions lying on this ellipse. The assumption being made is that particles outside this 2% area (i.e., larger x_0 , y_0) will be extracted on average in an equivalent or smaller number of turns; particles inside this area we shall ignore for the present. In a similar fashion to that described earlier in the report we have picked three extreme points on the ellipse. The results of the calculations are summarized in Table I.

Table I.

Initial Values		Number of Turns To Septum	
x mms	\dot{x} mrad	Calculated	Computer
0.73	-0.008	11	11
0.163	-0.001	15	17
-0.055	0.002	15	17

These results were obtained with a pulsed quadrupole field gradient at 120 g/cm. The agreement between the hand calculation and the computer simulation is good to within 2 turns, and in all cases the beam is extracted well within 1 ms (50 turns) for the maximum design pulsed quadrupole field strength.

Using a constant field strength in the above calculations is equivalent to assuming a square wave current pulse on the fast quadrupoles. This idealized situation can not be realized in practice, and a half sine wave pulse gives a much better approximation to the real world as demonstrated by Fig. 18 which shows the present Main Ring fast quadrupole current pulse. A detailed calculation of the time structure of the extracted beam generated by a pulse such as this requires a Monte-Carlo type program which we have not yet completed. In order, however, to get some feeling for how the extraction time varies with quadrupole field strength we have picked one point from the 2% phase space ellipse and calculated the number of turns before that particle reaches the electrostatic septum for three different values of the pulsed quadrupole field strength. The results are summarized in Table II.

Table II.

Quadrupole Field Gradient	Number of Turns To Septum
	Calculated
40 g/cm	21
80 g/cm	13
120 g/cm	11

$$x = 0.73 \text{ mms}$$
$$x' = -0.008 \text{ mrads}$$

Again we see good agreement between the analytic calculation and the computer simulation. The important thing to note however is the fact that the extraction time does not vary drastically with quadrupole field strength.

I would like to acknowledge many helpful discussions with Don Edwards of the Theory Group on the topics discussed in these design reports.

9-FEB-79 13:29
0.50 CMS PER DIV
HORIZONTAL PHASE SPACE
TUNE 19.45000
BETA 226.2759
ALPHA 3.03000

POSITION(MMS)

JUD1	B	807.20	0.00116
JUD1	D	807.20	0.00116
JUD1	F	807.20	0.00116
JUD2	A	807.20-0	0.00116
JUD2	C	807.20-0	0.00116
JUD2	E	807.20-0	0.00116
JCT1	B	807.30	2.00000
JCT1	D	807.30	2.00000
JCT1	F	807.30	2.00000
JCT2	A	807.30-2	0.00000
JCT2	C	807.30-2	0.00000
JCT2	E	807.30-2	0.00000

NORMALISED PHASE SPACE

BETA-THETA(MMS)

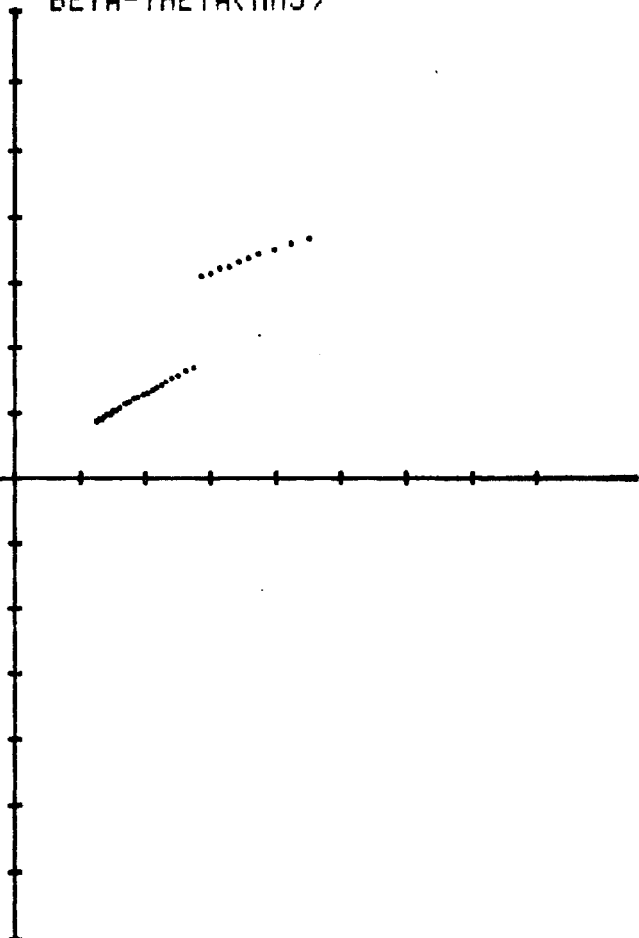


Fig. 1. Slow extraction septum offset 14 mms.

20-JAN-79 15:05
0.10 CMS PER DIV
HORIZONTAL PHASE SPACE
TUNE 19.45000
BETA 102.1730
ALPHA 1.89660

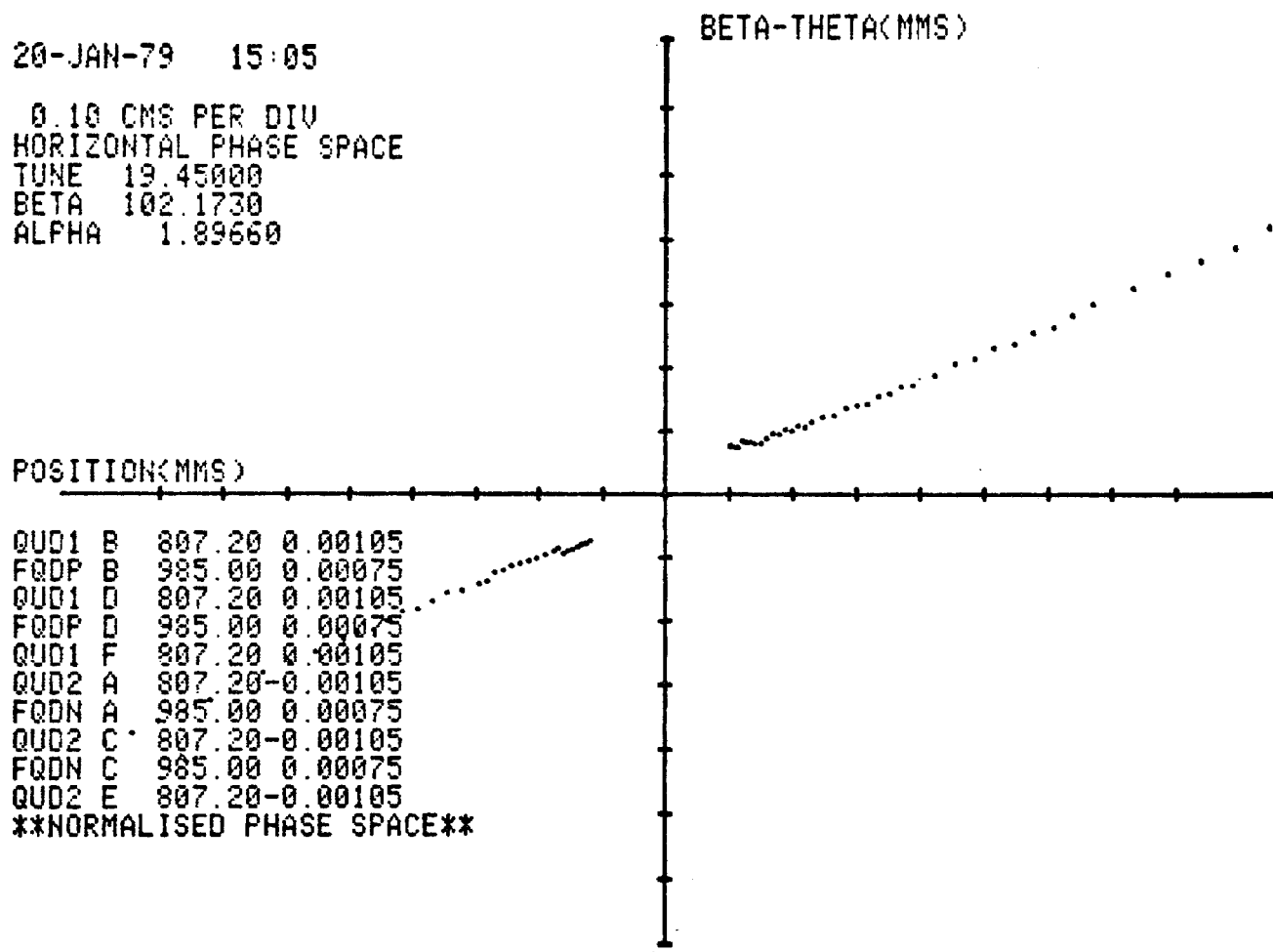


Fig. 2. Fast extraction phase space extremes
quad strength 120 g/cm $x_I^t = 1.0$ mm; $x_I^{t'} = -11 \mu\text{rad}$.

20-JAN-79 15:39

0.10 CMS PER DIV
HORIZONTAL PHASE SPACE
TUNE 19.45000
BETA 102.1757
ALPHA 1.89660

POSITION(MMS)

RUD1 B 807.20 0.00105
EQDP B 985.00 0.00075
RUD1 D 807.20 0.00105
EQDP D 985.00 0.00075
RUD1 F 807.20 0.00105
RUD2 A 807.20-0.00105
EQDN A 985.00 0.00075
RUD2 C 807.20-0.00105
EQDN C 985.00 0.00075
RUD2 E 807.20-0.00105
NORMALISED PHASE SPACE

BETA-THETA(MMS)

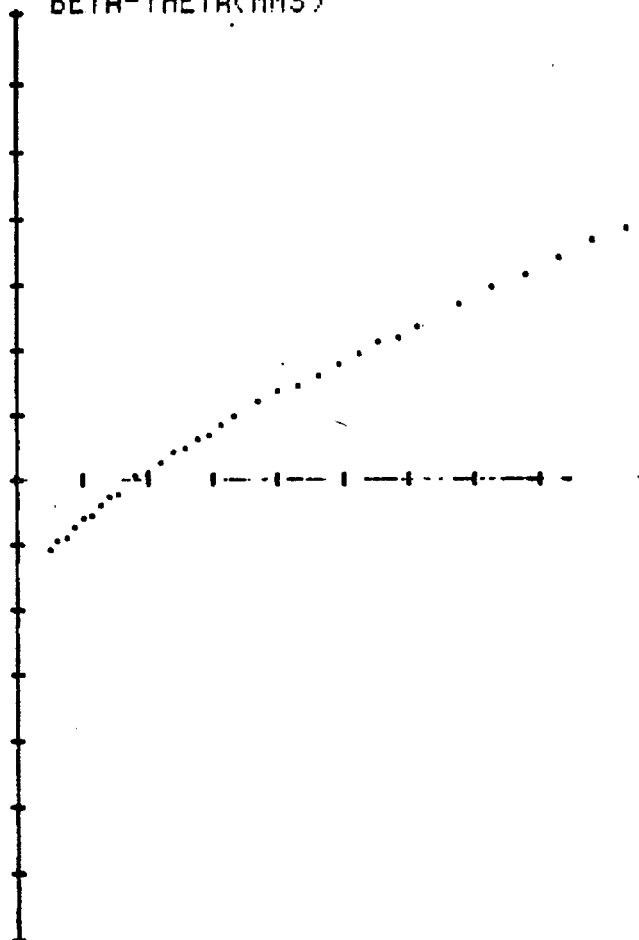


Fig. 3. Fast extraction phase space extremes
quad strength 120 g/cm $x_I = 0.5$ mm; $x'_I = -20 \mu\text{rad}$.

23-JAN-79 09:06

0.10 CMS PER DIV
HORIZONTAL PHASE SPACE
TUNE 19.45000
BETA 102.1736
ALPHA 1.89660

POSITION(MMS)

QU01 B 807.20 0.00105
FQDP B 985.00 0.00075
QU01 D 807.20 0.00105
FQDP D 985.00 0.00075
QU01 F 807.20 0.00105
QU02 A 807.20-0.00105
FQDN A 985.00 0.00075
QU02 G 807.20-0.00105
FQDN C 985.00 0.00075
QU02 E 807.20-0.00105
****NORMALISED PHASE SPACE****

BETA-THETA(MMS)

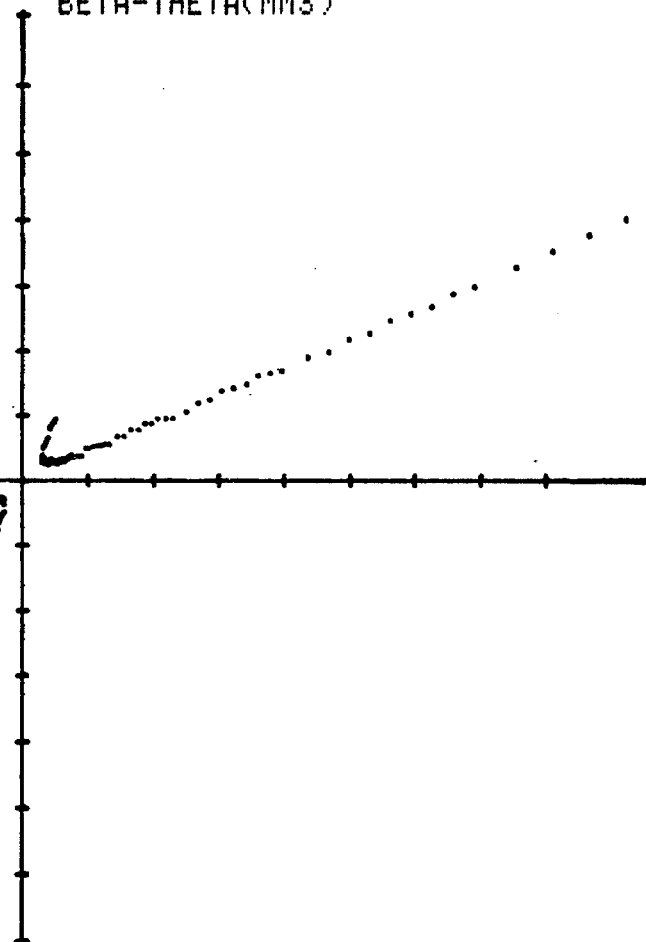


Fig. 4. Fast extraction phase space extremes
quad strength 120 g/cm $x_I = 0.5$ mm; $x'_I = 0.0 \mu\text{rad.}$

26-JAN-79 15:02
0.50 CMS PER DIV
HORIZONTAL PHASE SPACE
TUNE 19.45000
BETA 226.2724
ALPHA 3.03000

POSITION(MMS)

QU01 B	807.20	0.00105
FQDP B	985.00	0.00075
QU01 D	807.20	0.00105
FQDP D	985.00	0.00075
QU01 F	807.20	0.00105
QU02 A	807.20-0.00105	
FQDN A	985.00	0.00075
QU02 C	807.20-0.00105	
FQDN C	985.00	0.00075
QU02 E	807.20-0.00105	

NORMALISED PHASE SPACE

BETA-THETA(MMS)

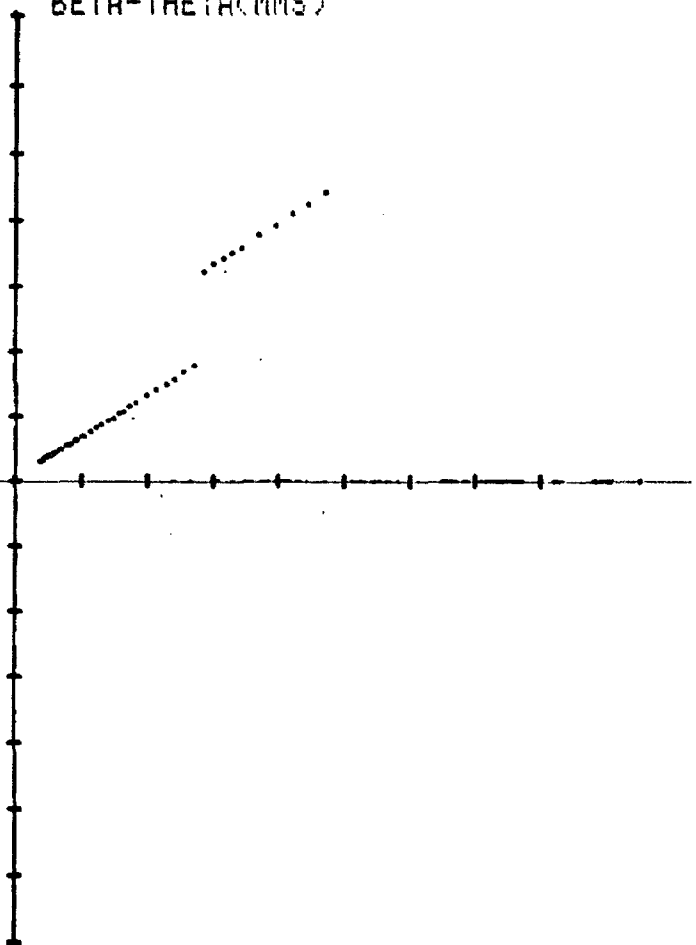


Fig. 5

20-JAN-79 15:37

0.50 CMS PER DIV
HORIZONTAL PHASE SPACE
TUNE 19.45000
BETA 226.2791
ALPHA 3.03000

POSITION(MMS)

QUD1 B	807.20	0.00105
FQDP B	985.00	0.00075
QUD1 D	807.20	0.00105
FQDP D	985.00	0.00075
QUD1 F	807.20	0.00105
QUD2 A	807.20-0	0.00105
FQDN A	985.00	0.00075
QUD2 C	807.20-0	0.00105
FQDN C	985.00	0.00075
QUD2 E	807.20-0	0.00105

NORMALISED PHASE SPACE

BETA-THETA(MMS)

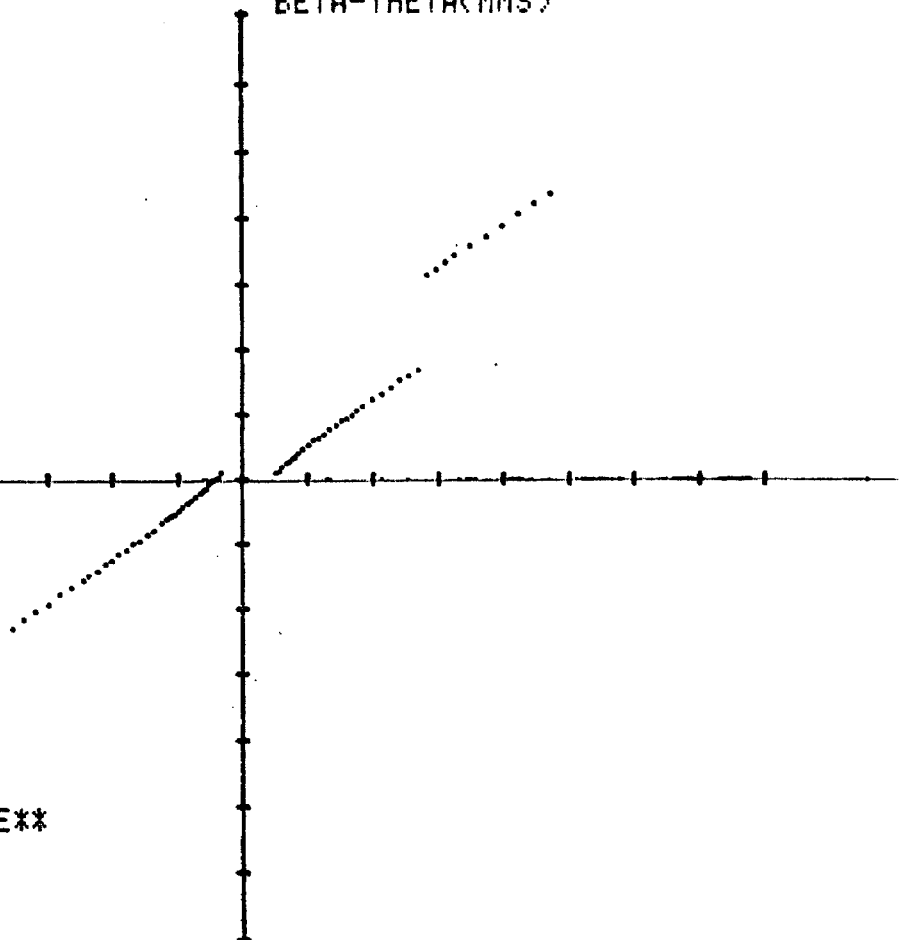


Fig. 6

23-JAN-79 08:58
0.50 CMS PER DIV
HORIZONTAL PHASE SPACE
TUNE 19.45000
BETA 226.2735
ALPHA 3.03000

POSITION(MMS)

QUD1	B	807.20	0.00105
FQDP	B	985.00	0.00075
QUD1	D	807.20	0.00105
FQDP	D	985.00	0.00075
QUD1	F	807.20	0.00105
QUD2	A	807.20-0.00105	
FQDN	A	985.00	0.00075
QUD2	C	807.20-0.00105	
FQDN	C	985.00	0.00075
QUD2	E	807.20-0.00105	

NORMALISED PHASE SPACE

BETA-THETA(MMS)

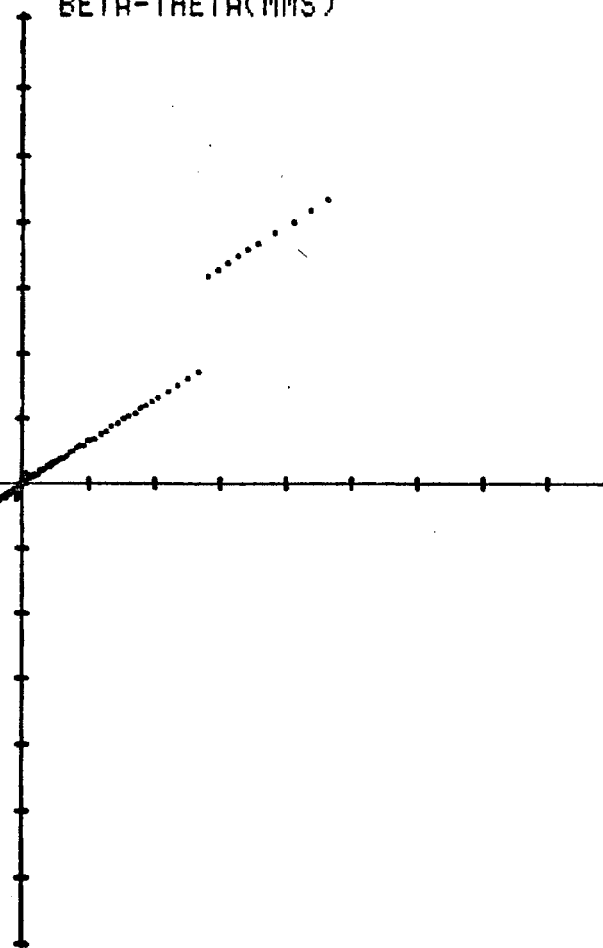


Fig. 7

16-DEC-78 16:14

0.58 CMS PER DIV
HORIZONTAL PHASE SPACE
TUNE 13.45000
BETA 226.2820
ALPHA 3.03010

POSITION(MMS)

QUD1 B	807.20	0.00105
FQDP B	985.00	0.00025
QUD1 D	807.20	0.00105
FQDP D	985.00	0.00025
QUD1 F	807.20	0.00105
QUD2 A	807.20-0	0.00105
FQDN A	985.00	0.00025
QUD2 C	807.20-0	0.00105
FQDN C	985.00	0.00025
QUD2 E	807.20-0	0.00105
OCT1 B	807.30	2.00000
OCT1 D	807.30	2.00000
OCT1 F	807.30	2.00000
OCT2 A	807.30-2	0.00000
OCT2 C	807.30-2	0.00000
OCT2 E	807.30-2	0.00000

NORMALISED PHASE SPACE

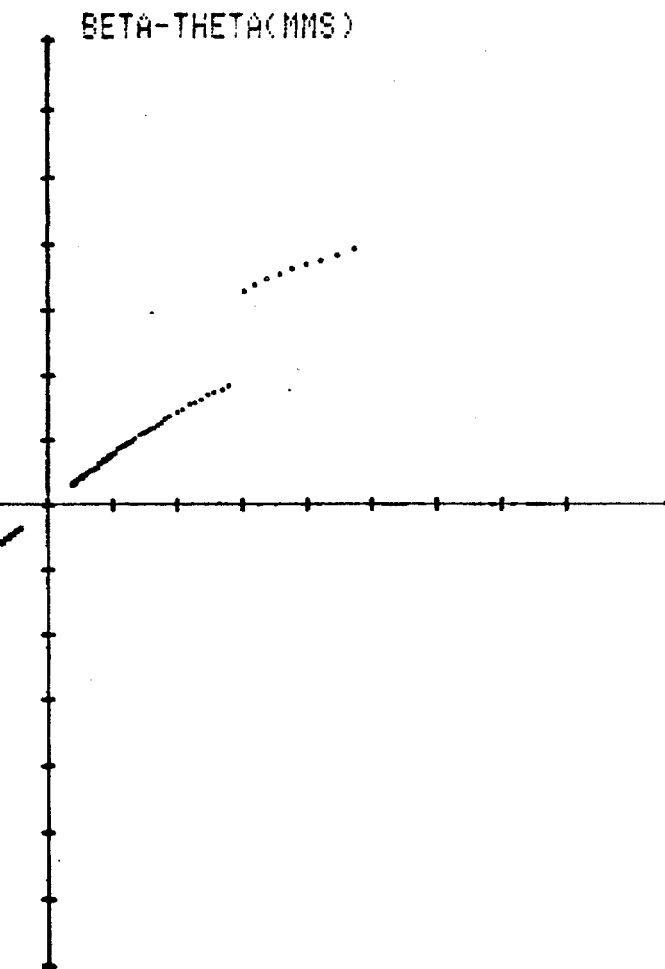


Fig. 8. Fast extraction septum offset 14 mms.
Quad strength 40 g/cm.

16-DEC-78 16:03

0.50 CMS PER DIV
HORIZONTAL PHASE SPACE
TUNE 13.45000
BETA 226.2710
ALPHA 3.03000

POSITION(MMS)

	B	D	F	A	C	E	B	D	F	A	C	E
RUD1	807.20	807.20	807.20	807.20	807.20	807.20	807.20	807.20	807.20	807.20	807.20	807.20
FODP	985.00	985.00	985.00	985.00	985.00	985.00	985.00	985.00	985.00	985.00	985.00	985.00
DUD1	0	0	0	0	0	0	0	0	0	0	0	0
FODP	0	0	0	0	0	0	0	0	0	0	0	0
RUD1	0	0	0	0	0	0	0	0	0	0	0	0
FODN	0	0	0	0	0	0	0	0	0	0	0	0
DUD2	0	0	0	0	0	0	0	0	0	0	0	0
FODN	0	0	0	0	0	0	0	0	0	0	0	0
RUD2	0	0	0	0	0	0	0	0	0	0	0	0
FODP	0	0	0	0	0	0	0	0	0	0	0	0
DCT1	B	D	F	A	C	E	B	D	F	A	C	E
DCT1	807.30	807.30	807.30	807.30	807.30	807.30	807.30	807.30	807.30	807.30	807.30	807.30
DCT1	2	2	2	2	2	2	2	2	2	2	2	2
DCT2	A	C	E	B	D	F	A	C	E	B	D	F
DCT2	807.30	807.30	807.30	807.30	807.30	807.30	807.30	807.30	807.30	807.30	807.30	807.30
DCT2	-2	-2	-2	-2	-2	-2	-2	-2	-2	-2	-2	-2

NORMALISED PHASE SPACE

BETA-THETA(MMS)

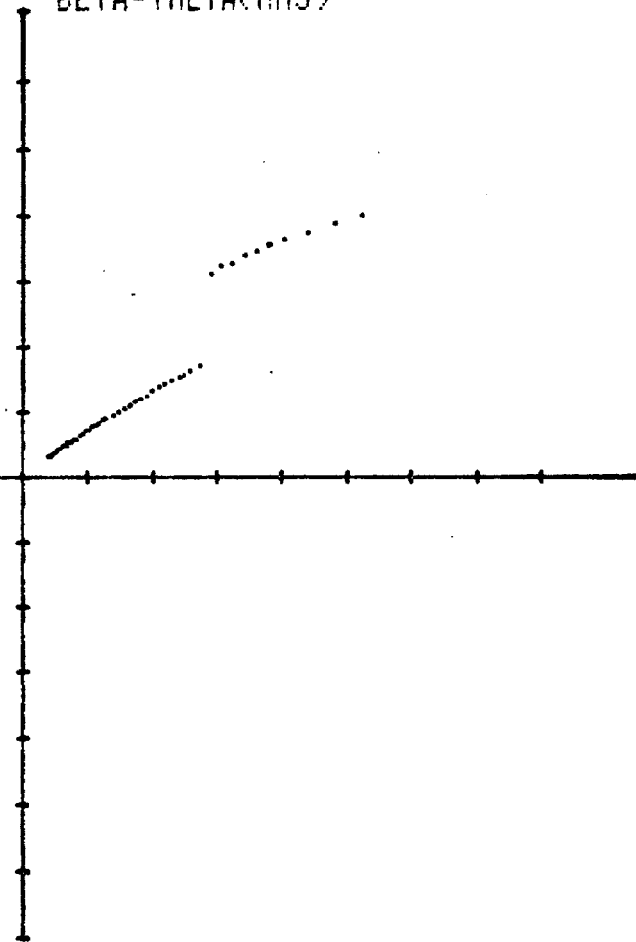


Fig. 9. Fast extraction septum offset 14 mms.
Quad strength 80 g/cm.

16-DEC-78 15:51

0.50 CMS PER DIV
HORIZONTAL PHASE SPACE
TUNE 19.45000
BETA 226.2745
ALPHA 3.03000

POSITION(MMS)

QUD1	B	807.20	0.00105
FQDP	B	985.00	0.00075
QUD1	D	807.20	0.00105
FQDP	D	985.00	0.00075
QUD1	F	807.20	0.00105
QUD2	A	807.20-0.00105	
FQDN	A	985.00	0.00075
QUD2	C	807.20-0.00105	
FQDN	C	985.00	0.00075
QUD2	E	807.20-0.00105	
OCT1	B	807.30	2.00000
OCT1	D	807.30	2.00000
OCT1	F	807.30	2.00000
OCT2	A	807.30-2.00000	
OCT2	C	807.30-2.00000	
OCT2	E	807.30-2.00000	

NORMALISED PHASE SPACE

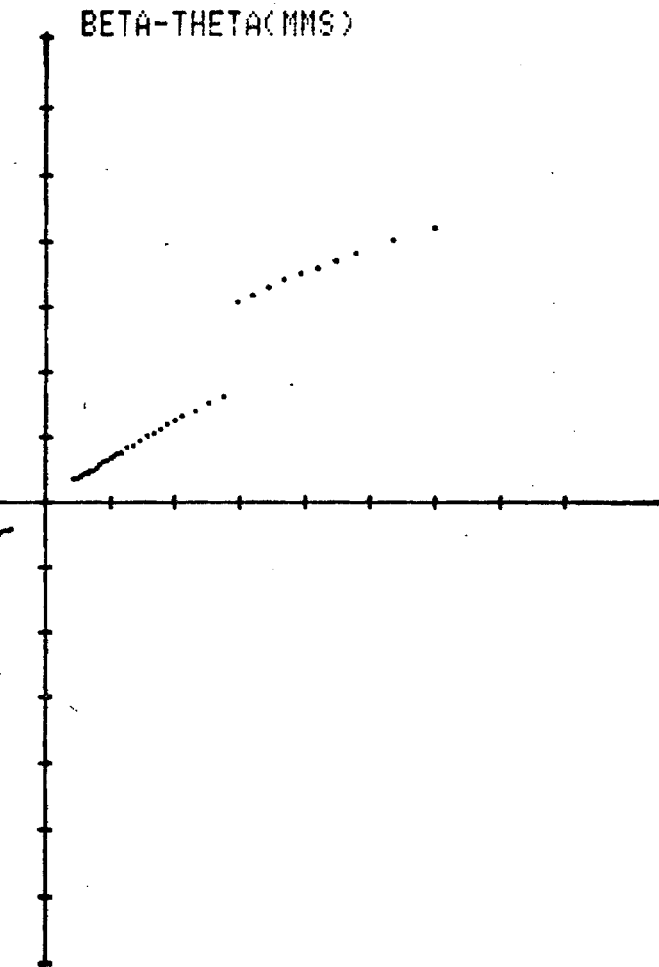


Fig. 10. Fast extraction septum offset 14 mms.
Quad strength 120 g/cm.

12-FEB-79 09:33

0.50 CMS PER DIV
HORIZONTAL PHASE SPACE
TUNE 19.45000
BETA 226.2791
ALPHA 3.03010

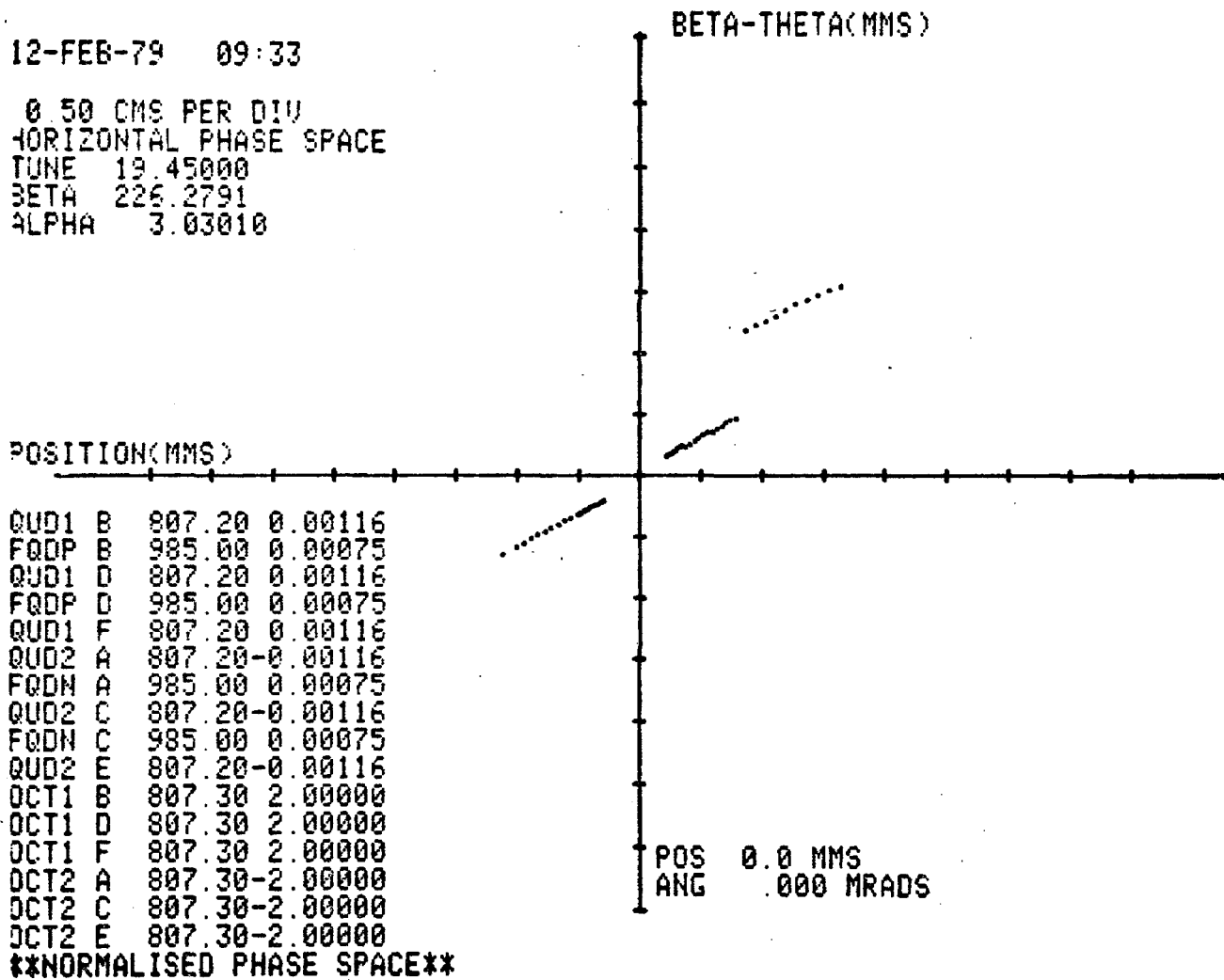


Fig. 11. Fast extraction septum offset 8 mm.
Quad strength 120 g/cm.

11-FEB-79 10:30

0.50 CMS PER DIV
HORIZONTAL PHASE SPACE
TUNE 19.45000
BETA 226.2791
ALPHA 3.03010

POSITION(MMS)

QUD1	B	807.20	0.00116
FQDP	B	985.00	0.00075
QUD1	D	807.20	0.00116
FQDP	D	985.00	0.00075
QUD1	F	807.20	0.00116
QUD2	A	807.20-0	0.00116
FQDN	A	985.00	0.00075
QUD2	C	807.20-0	0.00116
FQDN	C	985.00	0.00075
QUD2	E	807.20-0	0.00116
OCT1	B	807.30	2.00000
OCT1	D	807.30	2.00000
OCT1	F	807.30	2.00000
OCT2	A	807.30-2	0.00000
OCT2	C	807.30-2	0.00000
OCT2	E	807.30-2	0.00000

NORMALISED PHASE SPACE

BETA-THETA(MMS)

POS 6.0 MMS
ANG .015 MRADS

Fig. 12. Fast extraction septum offset 14 mms.
Quad strength 120 g/cm.

9-FEB-79 16:38
0.50 CMS PER DIV
HORIZONTAL PHASE SPACE
TUNE 19.45000
BETA 226.2771
ALPHA 3.03000

POSITION(MMS)

QUD1 B	807.20	0.00116
FQDP B	985.00	0.00025
QUD1 D	807.20	0.00116
FQDP D	985.00	0.00025
QUD1 F	807.20	0.00116
QUD2 A	807.20-0	0.00116
FQDN A	985.00	0.00025
QUD2 C	807.20-0	0.00116
FQDN C	985.00	0.00025
QUD2 E	807.20-0	0.00116
OCT1 B	807.30	2.00000
OCT1 D	807.30	2.00000
OCT1 F	807.30	2.00000
OCT2 A	807.30-2	0.00000
OCT2 C	807.30-2	0.00000
OCT2 E	807.30-2	0.00000

NORMALISED PHASE SPACE

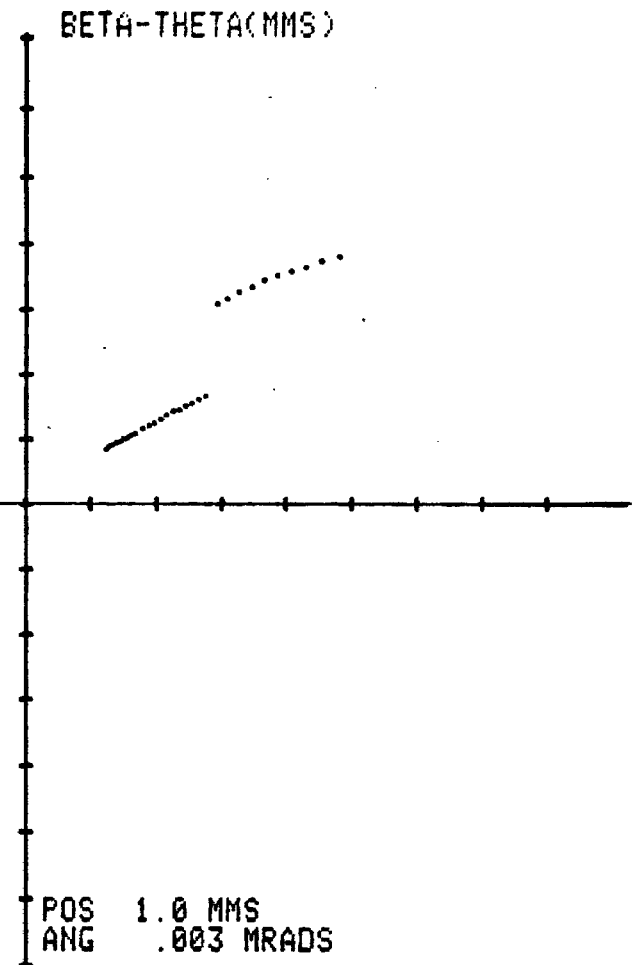


Fig. 13. Fast extraction septum offset 14 mms.
Quad strength 40 g/cm.

11-FEB-79 10:47
0.50 CMS PER DIV
HORIZONTAL PHASE SPACE
TUNE 19.45000
BETA 226.2794
ALPHA 3.03010

POSITION(MMS)

QU01 B	807.20	0.00116
FQDP B	985.00	0.00050
QU01 D	807.20	0.00116
FQDP D	985.00	0.00050
QU01 F	807.20	0.00116
QU02 A	807.20-0	0.00116
FQDN A	985.00	0.00050
QU02 C	807.20-0	0.00116
FQDN C	985.00	0.00050
QU02 E	807.20-0	0.00116
OCT1 B	807.30 2	0.00000
OCT1 D	807.30 2	0.00000
OCT1 F	807.30 2	0.00000
OCT2 A	807.30-2	0.00000
OCT2 C	807.30-2	0.00000
OCT2 E	807.30-2	0.00000

NORMALISED PHASE SPACE

BETA-THETA(MMS)

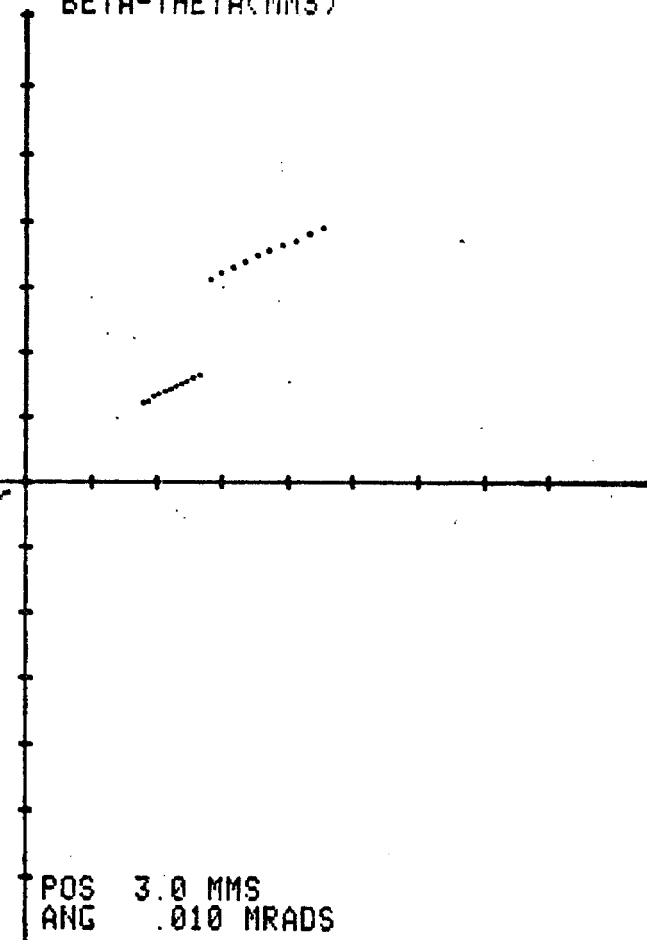


Fig. 14. Fast extraction septum offset.
Quad strength 80 g/cm.

9-FEB-79 13:29

0.50 CMS PER DIV
HORIZONTAL PHASE SPACE
TUNE 19.45000
BETA 226.2759
ALPHA 3.03000

POSITION(MMS)

DUD1	B	807.20	0.00116
DUD1	D	807.20	0.00116
DUD1	F	807.20	0.00116
DUD2	A	807.20-0	0.00116
DUD2	C	807.20-0	0.00116
DUD2	E	807.20-0	0.00116
DCT1	B	807.30	2.00000
DCT1	D	807.30	2.00000
DCT1	F	807.30	2.00000
DCT2	A	807.30-2	0.00000
DCT2	C	807.30-2	0.00000
DCT2	E	807.30-2	0.00000

NORMALISED PHASE SPACE

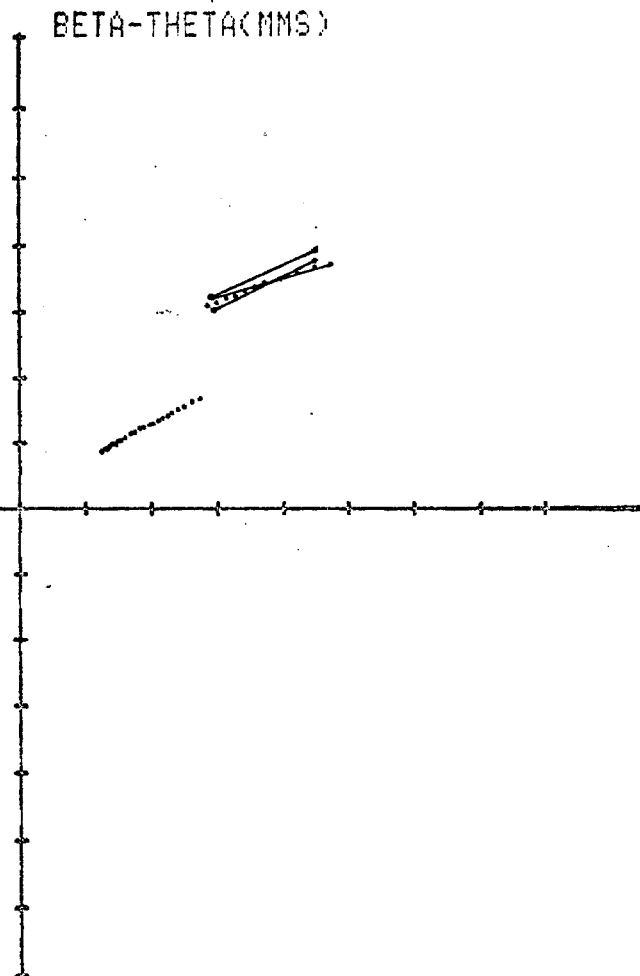


Fig. 15. Fast and slow extraction septum offset 14 mms.

12-FEB-79 11:19
0.50 CMS PER DIV
HORIZONTAL PHASE SPACE
TUNE 19.45000
BETA 226.2737
ALPHA 3.03000

POSITION(MMS)

QUD1	B	807.20	0.00116
FQDP	B	985.00	0.00050
QUD1	D	807.20	0.00116
FQDP	D	985.00	0.00050
QUD1	F	807.20	0.00116
QUD2	A	807.20-0.00116	
FQDN	A	985.00	0.00050
QUD2	C	807.20-0.00116	
FQDN	C	985.00	0.00050
QUD2	E	807.20-0.00116	
OCT1	B	807.30	2.00000
OCT1	D	807.30	2.00000
OCT1	F	807.30	2.00000
OCT2	A	807.30-2.00000	
OCT2	C	807.30-2.00000	
OCT2	E	807.30-2.00000	

NORMALISED PHASE SPACE

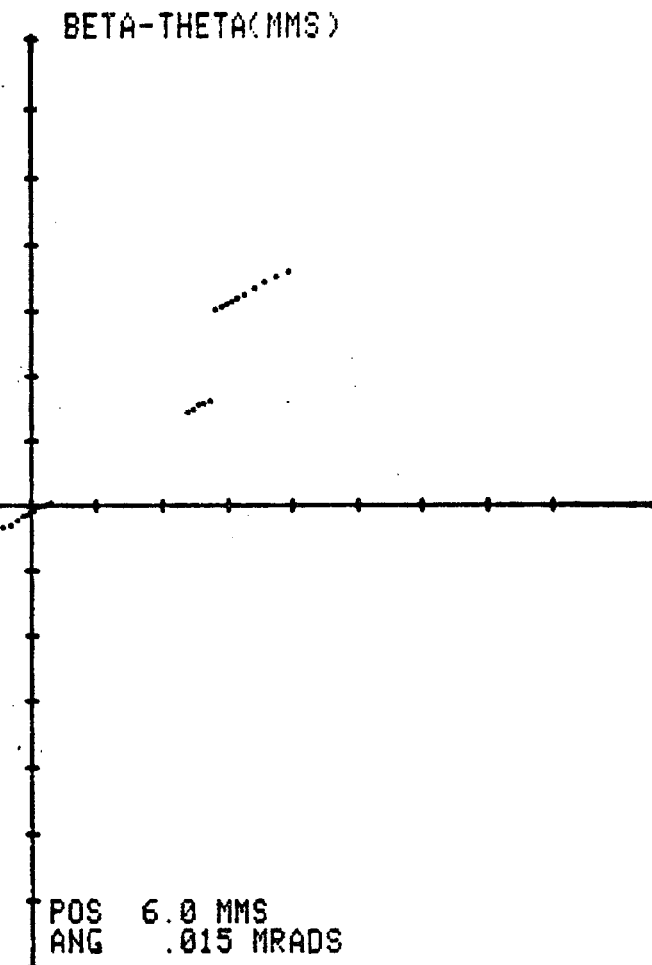


Fig. 16. Fast extraction septum offset 14 mms.
Quad strength 80 g/cm.

13-FEB-79 09:23

0.50 CMS PER DIV
HORIZONTAL PHASE SPACE
TUNE 19.45000
BETA 226.2794
ALPHA 3.03010

POSITION(MMS)

QUAD	POLE	X POSITION	Z POSITION
QUD1	B	807.20	0.00116
FQDP	B	985.00	0.00025
QUD1	D	807.20	0.00116
FQDP	D	985.00	0.00025
QUD1	F	807.20	0.00116
QUD2	A	807.20-0	0.00116
FQDN	A	985.00	0.00025
QUD2	C	807.20-0	0.00116
FQDN	C	985.00	0.00025
QUD2	E	807.20-0	0.00116
OCT1	B	807.30	2.00000
OCT1	D	807.30	2.00000
OCT1	F	807.30	2.00000
OCT2	A	807.30-2	2.00000
OCT2	C	807.30-2	2.00000
OCT2	E	807.30-2	2.00000

NORMALISED PHASE SPACE

BETA-THETA(MMS)

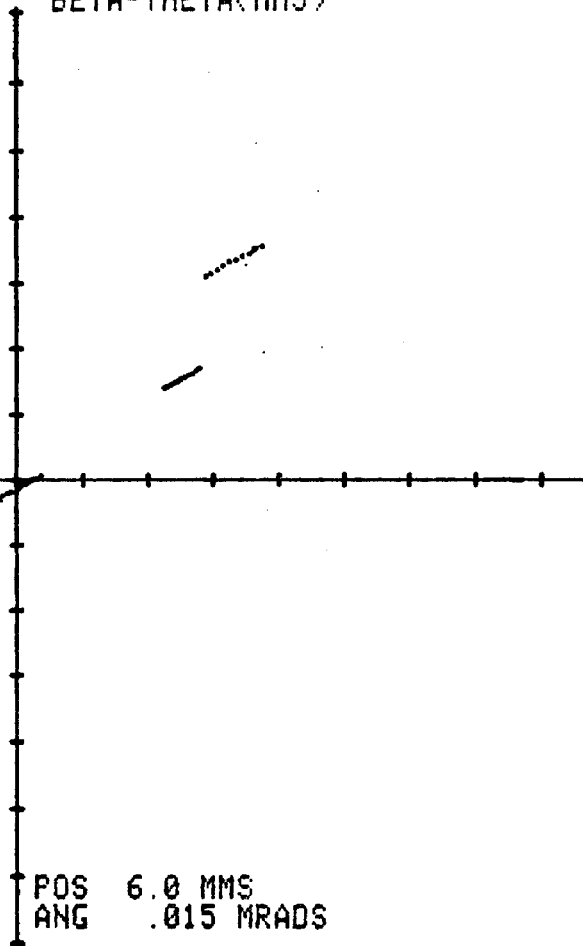


Fig. 17. Fast extraction septum offset 14 mms.
Quad strength 40 g/cm.

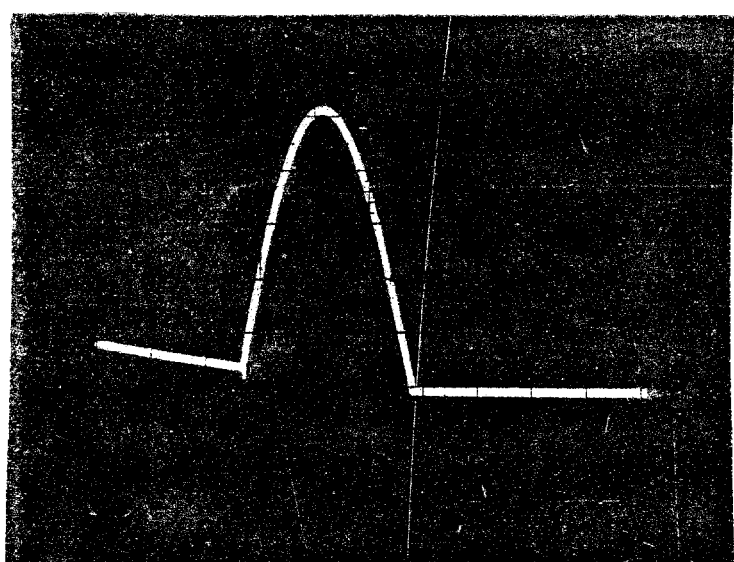


Fig. 18. Fast resonant extraction pulsed waveform.

December 13, 1978/D. A. Edwards

EFFECT OF A HIGH BETA INSERTION ON RESONANT
EXTRACTION FROM THE ENERGY DOUBLER

The electrostatic septum for extraction from the Doubler is to be located in straight section F, according to the present plan,¹ since a septum of sufficient strength cannot occupy the gap corresponding to the location of the main ring septum. Moreover, the septum will be well upstream of the center of straight section F to facilitate protection of the superconducting magnets in F sector from radiation caused by particles interacting in the septum.

Thus, the electrostatic septum finds itself in a region of rather low beta - some 50 m - in the horizontal plane for the standard main ring variety lattice. The magnetic septum in straight section A is also located at a beta of essentially the same magnitude.

An increase in the amplitude function at the electrostatic septum can lead to an improvement in the extraction efficiency. This effect is discussed below and is the main topic of these notes. Another important effect is that an increase in beta at the positions of both septa not only decreases the deflection necessary at the electrostatic element to achieve a particular offset at the magnetic septum, but if accompanied by a relative reduction in the vertical beta permits the latter element to be designed to operate at a higher field.

A modification of the lattice that produces a comparatively high beta at the upstream end of a long straight section has been devised by Collins.² Instead of 50 m, the amplitude function rises to approximately 225 m at the septum locations. In effect, a given electrostatic septum becomes stronger by a factor of 4-1/2. Though dilation of the angular width of the beam by $\sqrt{4.5}$ at the septum may reduce the gain, the improvement is still substantial. The vertical beta has decreased by more than a factor of 3, leading to a more favorable aspect ratio for the magnetic septum. These advantages of the high beta modification are relatively clear, and we turn to the discussion of extraction efficiency.

First, we need an expression for the efficiency, or, better, the inefficiency. If extraction proceeds so slowly as to be a steady-state process, the density of the outward bound particles will vary inversely as the rate of change of position; i.e.

$$N(x) \propto \frac{1}{dx/dn} .$$

Let x_s be the position of the upstream with respect to the central orbit, δ be the thickness of the septum wires, and Δ , the "step size", be the growth in x for a particle between the time it passes the septum with $x = x_s$ and its next encounter at the proper phase to enter the septum. Assuming that only the wires intercept particles, then the inefficiency ε can be defined as

$$\varepsilon = \frac{\int_{x_s}^{x_s + \delta} \frac{dx}{(dx/dn)}}{\int_{x_s}^{x_s + \Delta} \frac{dx}{(dx/dn)}}$$

Take the case of third integer extraction, and for the present suppose that the stable phase space is negligibly small - we'll go into the finite phase space case later. Then

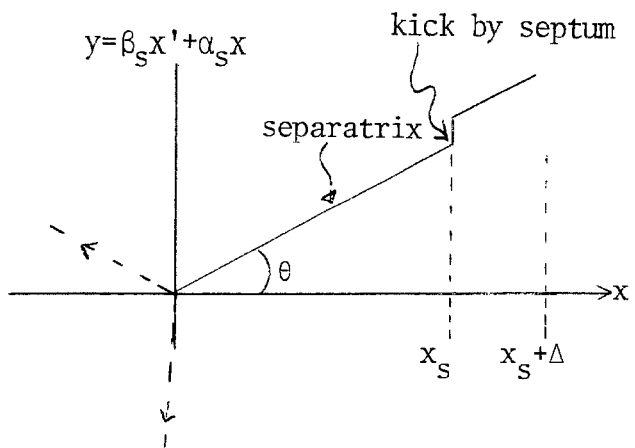
$$\frac{dx}{dn} \propto x^2 ,$$

and

$$\varepsilon = \delta \left(\frac{1}{x_s} + \frac{1}{\Delta} \right) ,$$

where we have made the approximation $\delta \ll x_s$.

Second, we must relate the maximum displacement at the upstream to the maximum displacement elsewhere in the machine. Presumably one doesn't want the latter quantity to exceed some limit. If the phase space at the electrostatic septum is as shown in the sketch, then the estimate of the maximum displacement x_{max} in



the body of the accelerator is

$$x_{\max} = \frac{x_s + \Delta}{\cos \theta} \left(\frac{\beta_c}{\beta_s} \right)^{1/2}$$

where β_c is the maximum beta in a standard cell, and β_s the value at the septum. For best efficiency, one would like θ to be as small as possible; an idea of how small it can be can be obtained by rotating the diagram clockwise by $\sim 80^\circ$ to see how the picture looks at the magnetic septum. Then the kick from the electrostatic septum is almost fully projected in the x -axis regardless of θ , but for $\theta = 0$ the magnetic septum would be in the middle of the aperture and, even if the stable phase space were truly negligible, would shadow one of the other outgoing separatrices shown as a dotted line in the sketch. Probably θ can be no smaller than $25-30^\circ$.

For given x_{\max} , β_c , β_s , θ , then $x_s + \Delta$ is fixed. The inefficiency can be written

$$\varepsilon = \delta \left[\frac{x_s + \Delta}{x_s \Delta} \right]$$

the minimum of which occurs when $x_s = \Delta = 1/2(x_s + \Delta)$, and

$$\varepsilon_{\min} = \frac{4\delta}{(x_s + \Delta)}$$

So improvement in efficiency is associated, not surprisingly, with increasing $(x_s + \Delta)$, which in turn varies as $\sqrt{\beta_s}$ for constant values of the other quantities.

Now consider two examples. In both, we take $x_{\max} = 20$ mm and $\beta_c = 100$ m. Let $\theta = 30^\circ$.

For the unmodified machine, $\beta_s \approx 50$ m, and

$$x_s + \Delta = 20 \frac{\sqrt{3}}{2} \frac{1}{\sqrt{2}} = 12.25 \text{ mm.}$$

The best efficiency one could hope for would have $x_s = \Delta = 6-1/8$ mm. The step size uses only $\sim 2/3$ of the septum aperture. Taking $\delta = 0.003"$ gives $\epsilon = 2.4\%$.

With the high beta:

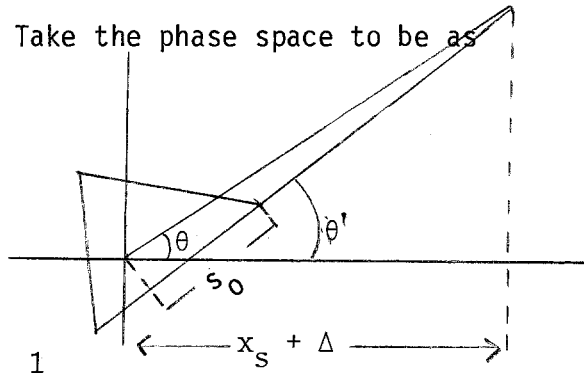
$$x_s + \Delta = 12.25 \text{ mm} \times \left(\frac{225}{50} \right)^{1/2} = 26 \text{ mm.}$$

Setting $\Delta = 10$ mm to match the existing septum design yields $\epsilon = 1.2\%$, an improvement of a factor of two. But now $x_s + \Delta$ exceeds the 20 mm limit. There are at least four options:

- (a) Claim that 26 mm is all right "just once."
- (b) Enlarge the magnets in the immediate neighborhood of the high beta.
- (c) Increase θ to 40° , making $(x_s + \Delta) = \sim 23$ mm at both septa, and say that excursion is tolerable.
- (d) Insist in maintaining the 20 mm limit; then $\epsilon_{\min} = 1.5\%$, and trust to luck to be able to do better by finding the limit is too small.

Introduction of a finite phase space mainly makes the algebra more complicated without changing the results by much. Take the phase space to be as shown in the sketch. Then the ratio of the inefficiency for emittance E to the ϵ_{\min} for vanishing emittance can be written

$$r = \frac{1}{2} \frac{s_{\max}}{x_{\max}} \frac{\cos\theta'}{\cos\theta} \frac{1}{(f-f_a)(f+f_b)} \frac{1}{\ln \left\{ \frac{1-f_a}{1+f_b} \frac{f+f_b}{f-f_a} \right\}}$$



$$\text{where } s_{\max} = \left(\frac{\beta_c E}{\sqrt{3}} \right)^{1/2}$$

$$\tan \theta' = \tan \theta + \frac{s_{\max} x_{\max}}{\sqrt{3} \cos \theta}$$

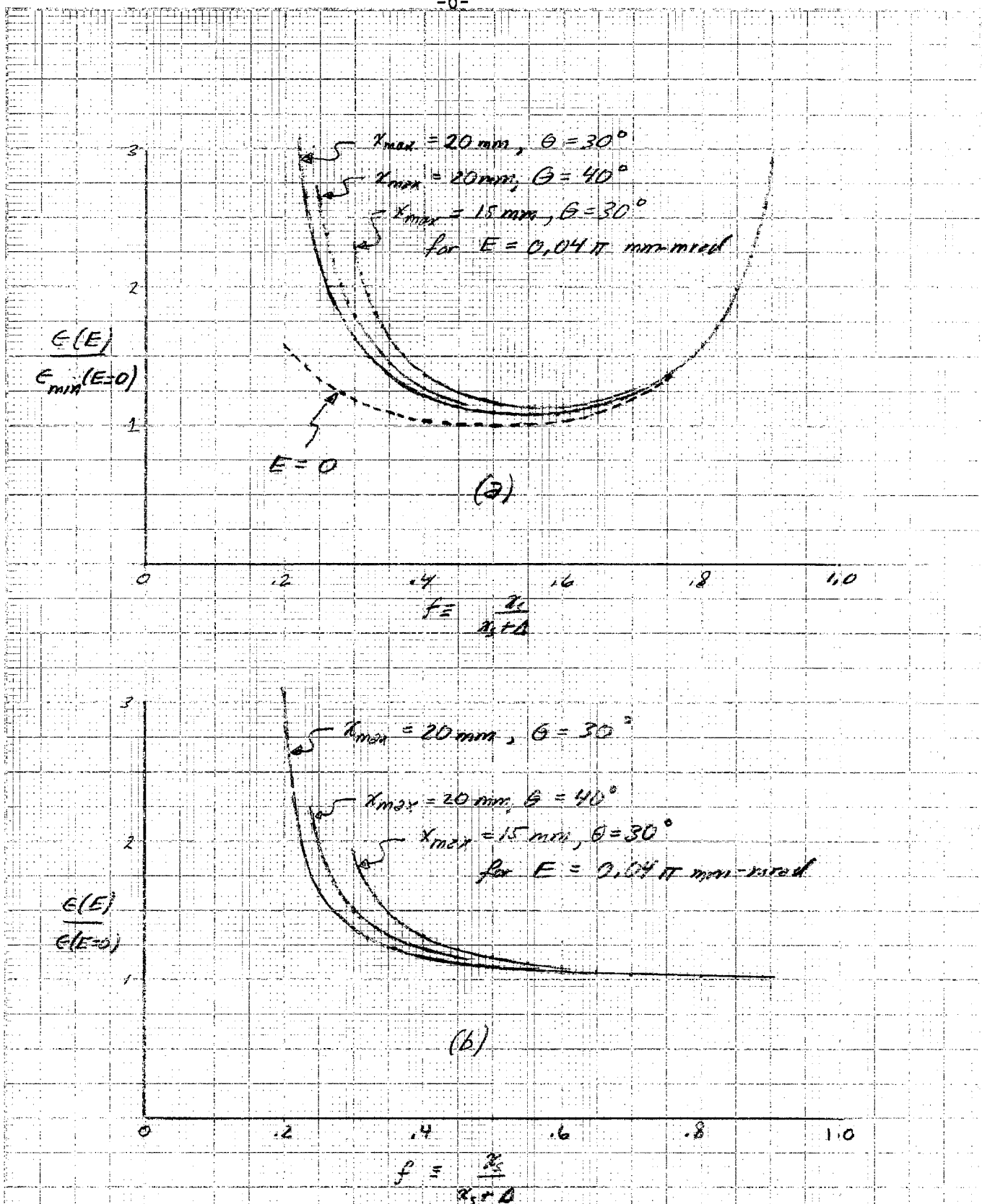
$$f_a = \frac{s_{\max} x_{\max}}{\sqrt{3} \cos \theta} (\cos \theta' + \sin \theta'), f_b = \frac{s_{\max} x_{\max}}{\sqrt{3} \cos \theta} (\cos \theta' - \sin \theta')$$

$$f = \frac{x_s}{s_x + \Delta}$$

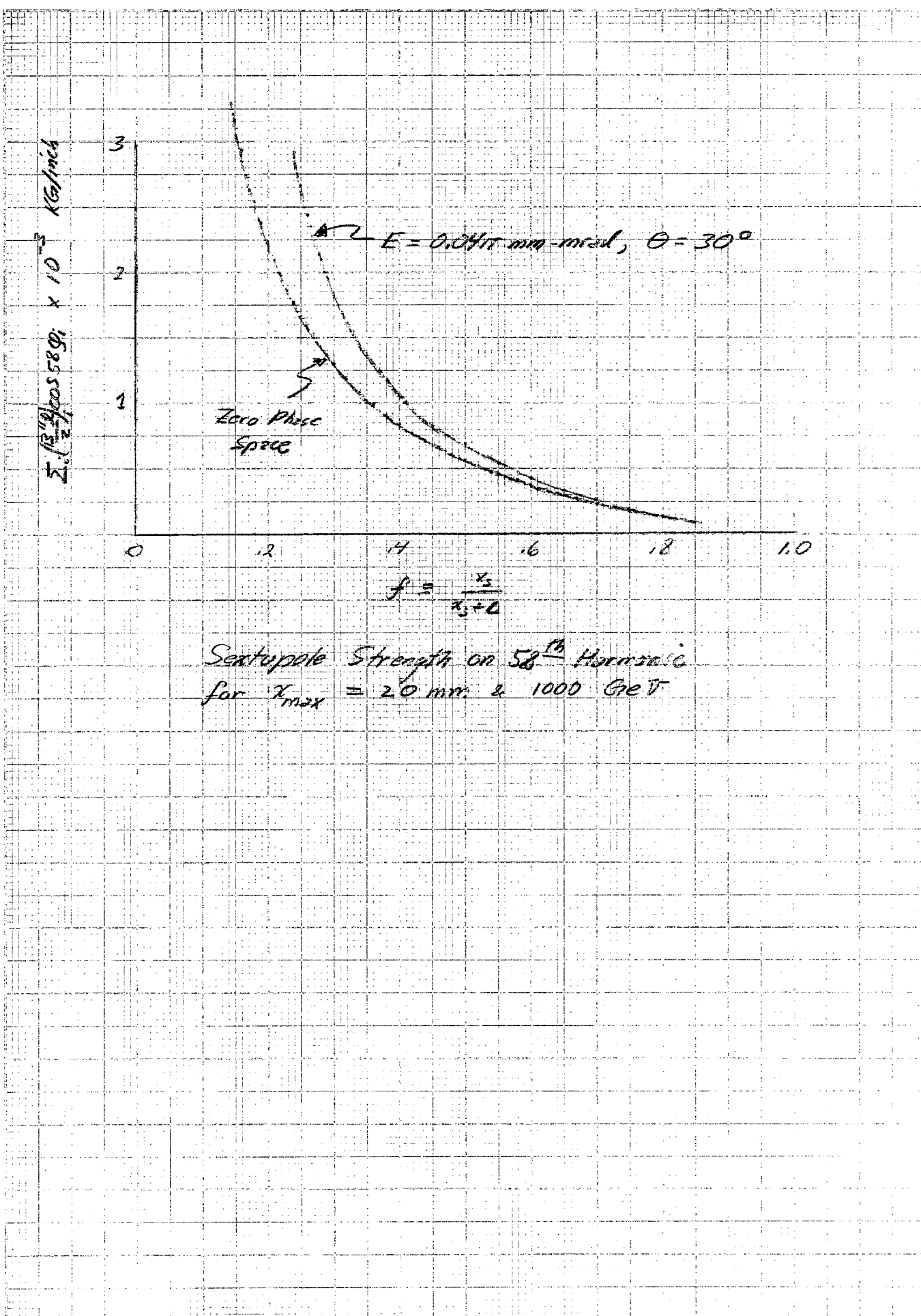
In the sketch, s_0 characterizes the stable area at the septum; s_{\max} is the corresponding quantity at β_c . Since β_s doesn't appear in the expression for r , the degradation in efficiency is factor to be applied independent of the high beta modification. For the emittance that we are dealing with (e.g., $E \sim 0.04\pi$ mm-mrad at ~ 400 GeV) the factor isn't large in any case. A few cases are plotted on the first of the graphs attached. The second shows the magnitudes of the sextupole coefficients that are required.

References:

1. L. C. Teng in "The Energy Doubler", Fermilab, June 1976.
2. T.L. Collins, UPC No. 14, November 14, 1978.

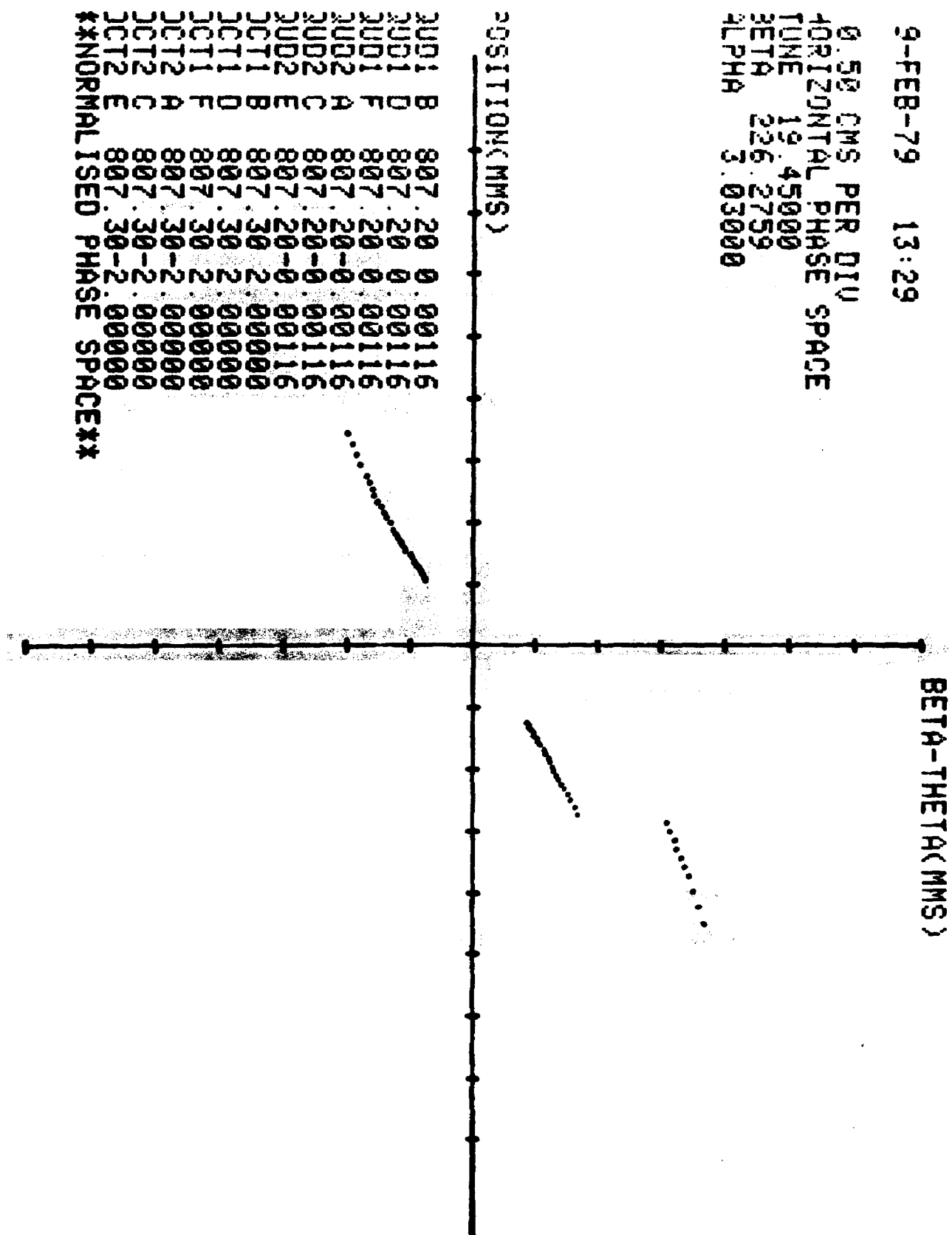


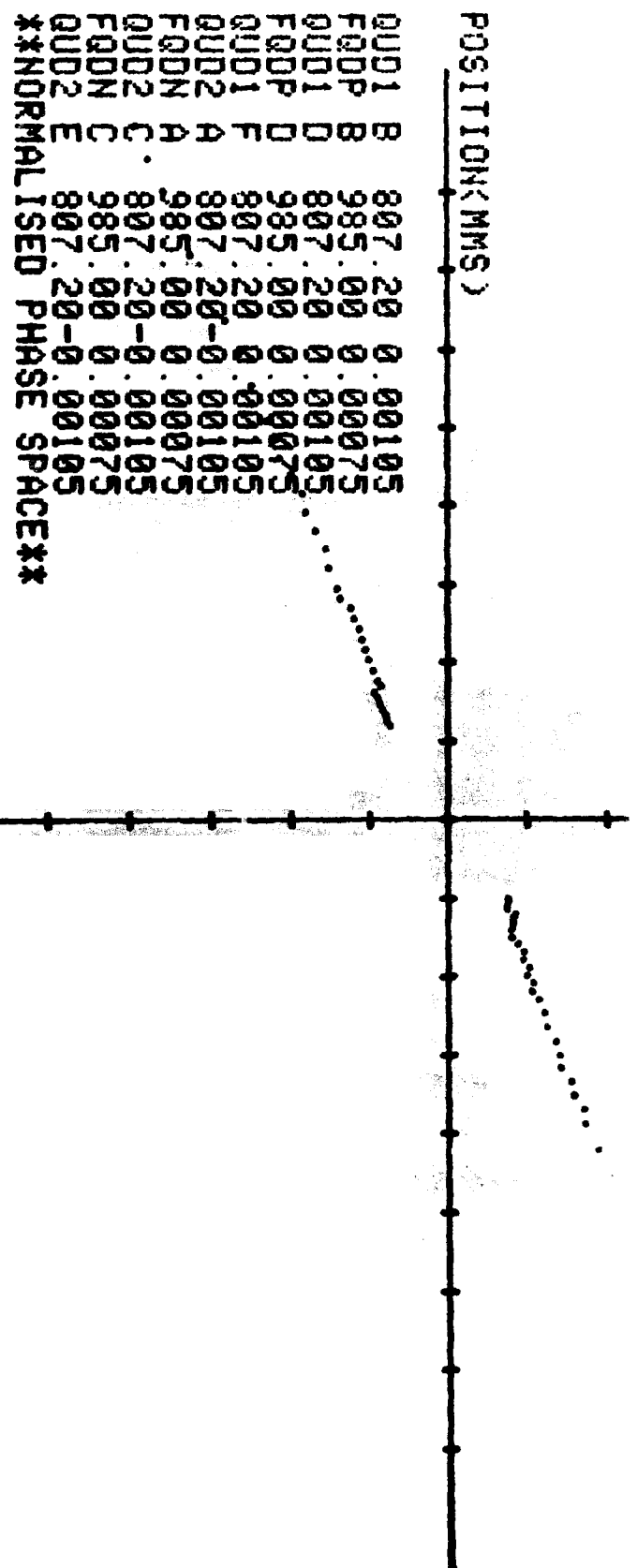
Inefficiencies for emittance E (a) relative to minimum inefficiency for $E=0$, and (b) relative to inefficiency for $E=0$ at same f .



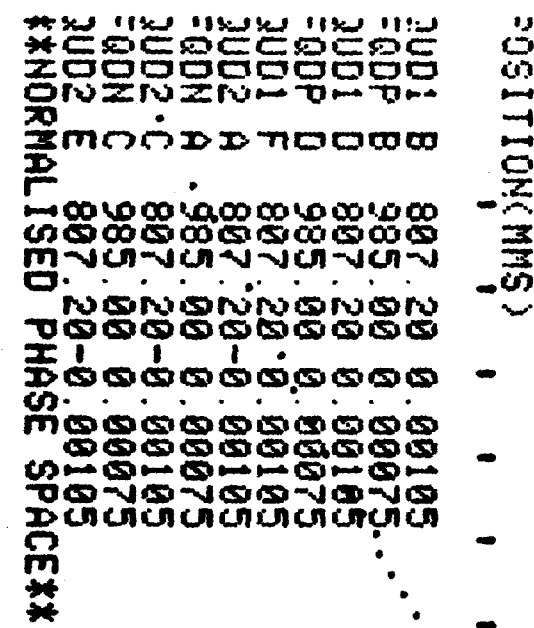
9-FEB-79 13:29

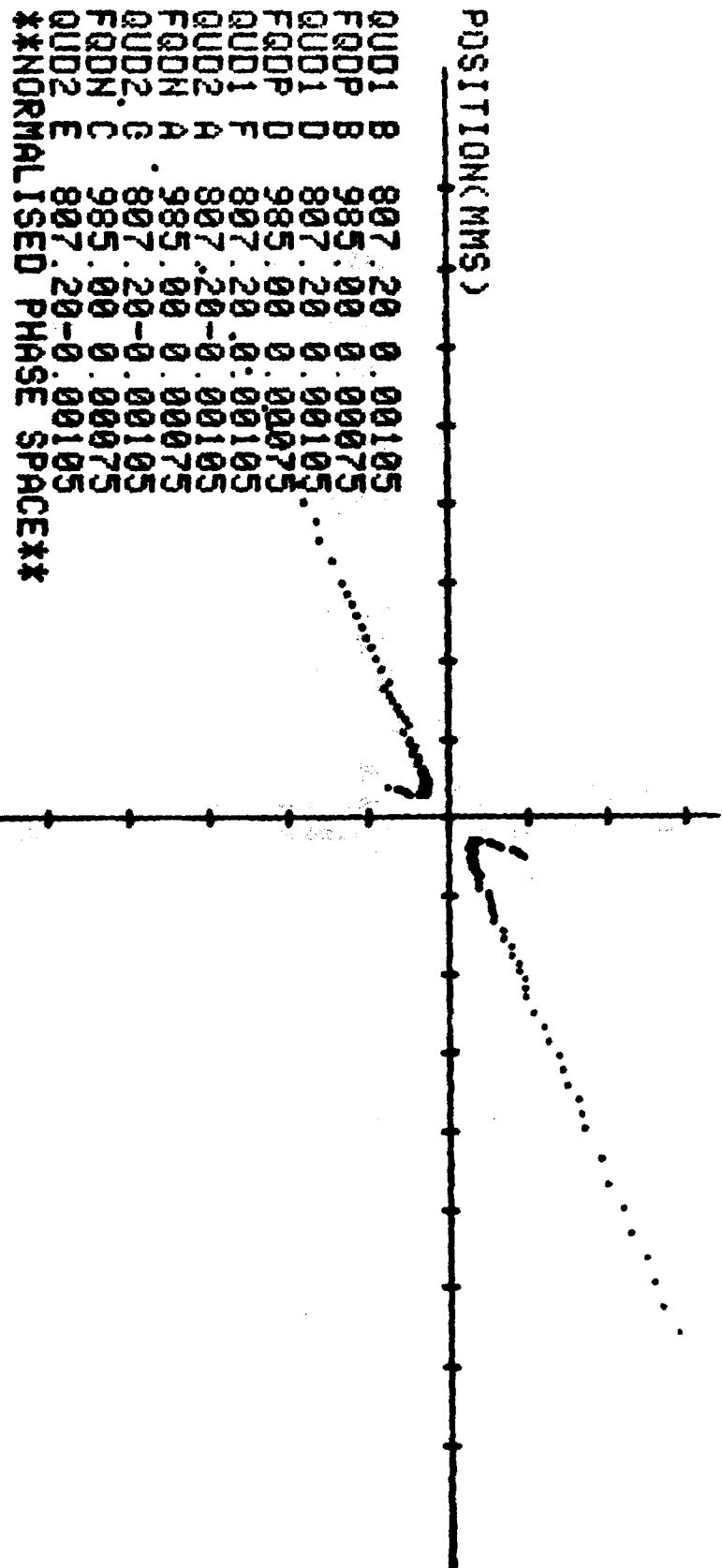
BETÀ-THETAC(MMS)

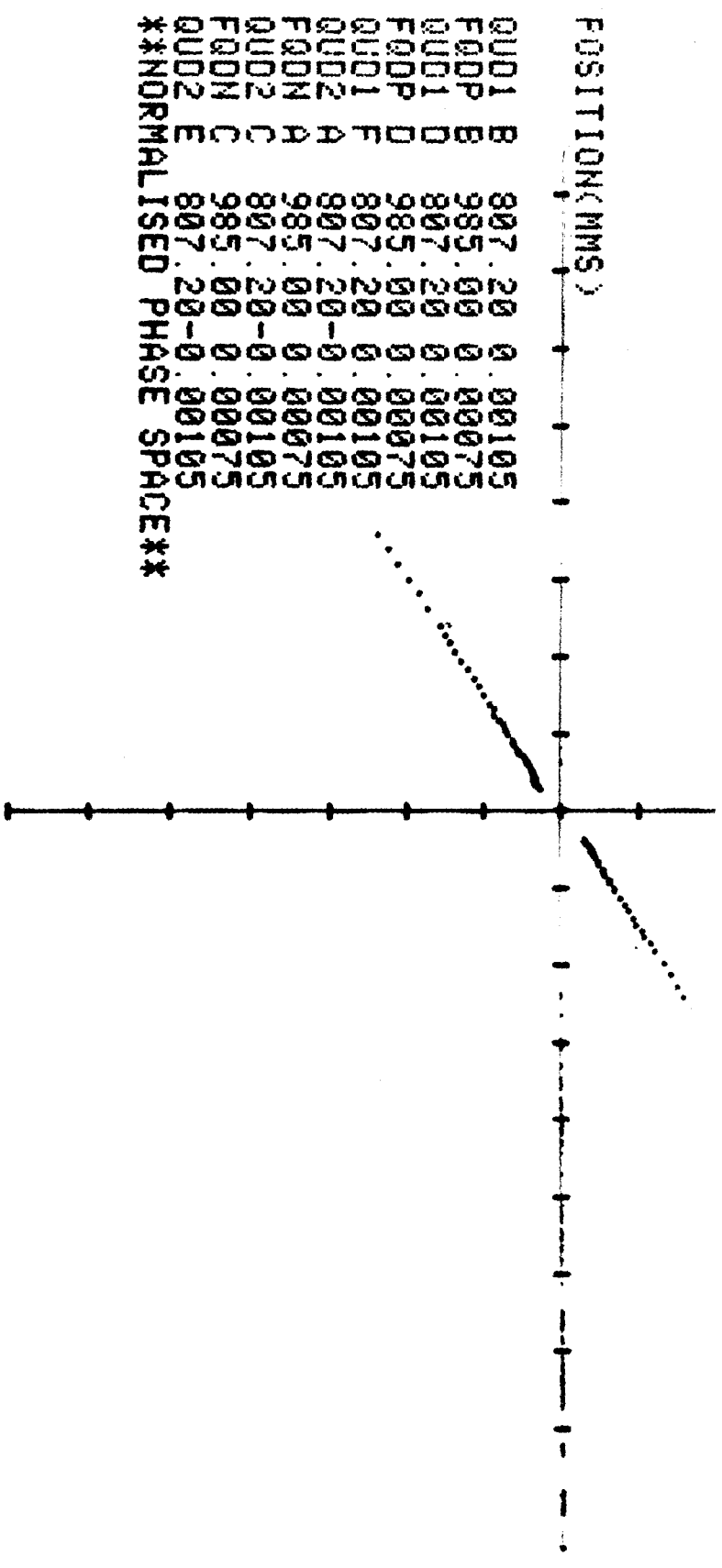




DELTA LOR 1-89660



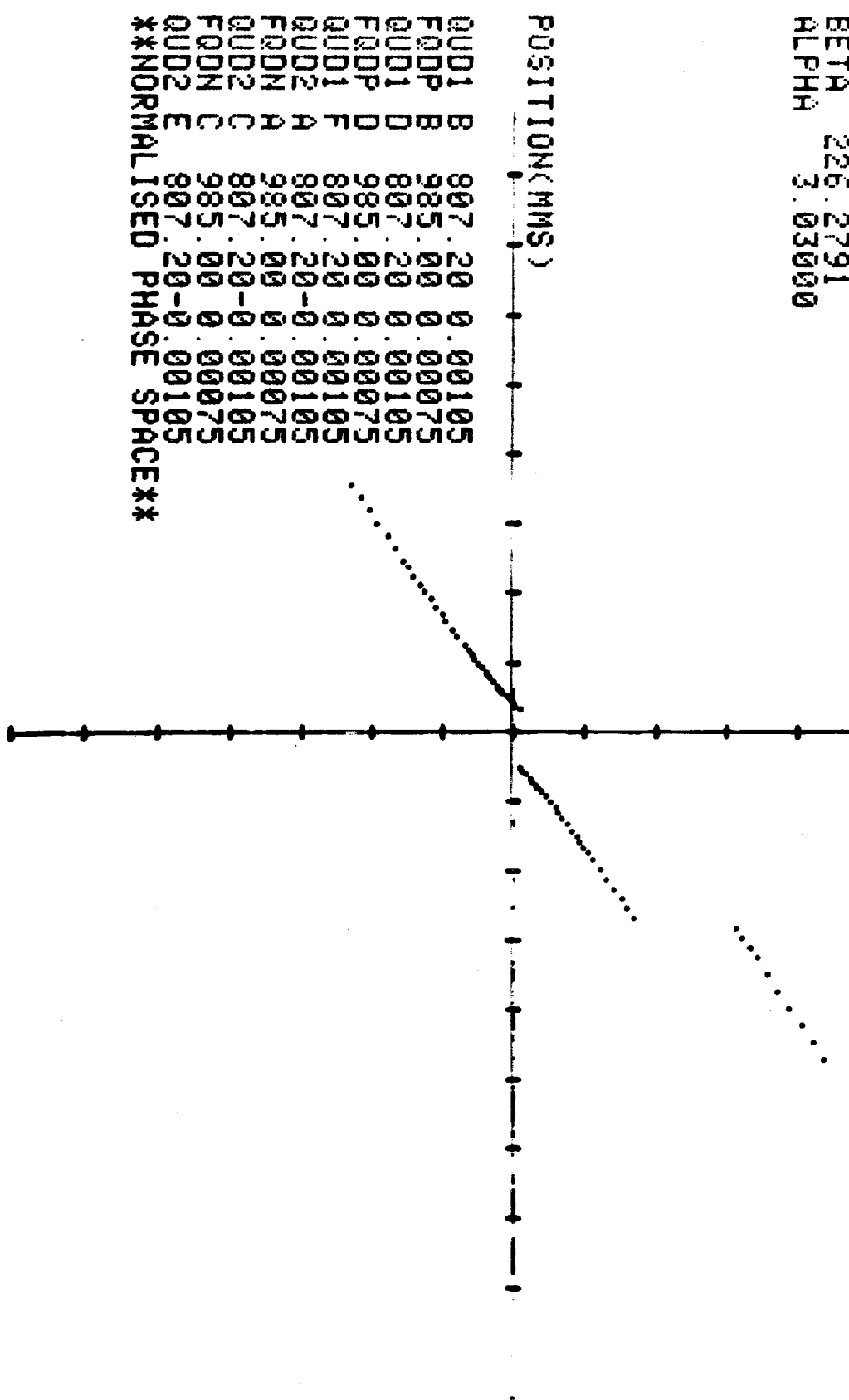




20-JAN-79 15:37

BETA-THETA(MMS)

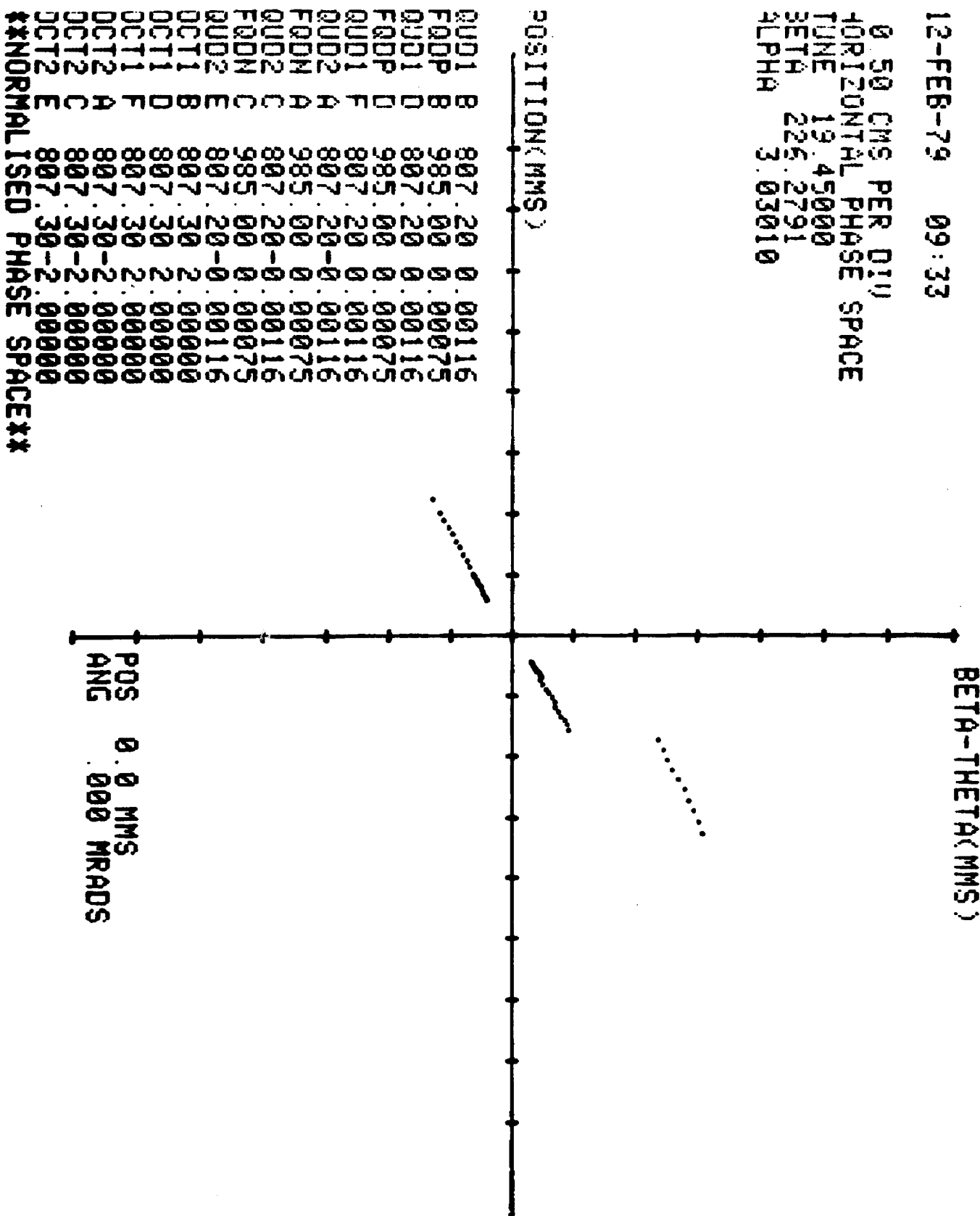
0.50 CMS PER DIV
HORIZONTAL PHASE SPACE
TUNE 19.45000
BETA 226.2791
ALPHA 3.03000



12-FEB-79
99 : 33

BETA-THETAC(MMS)

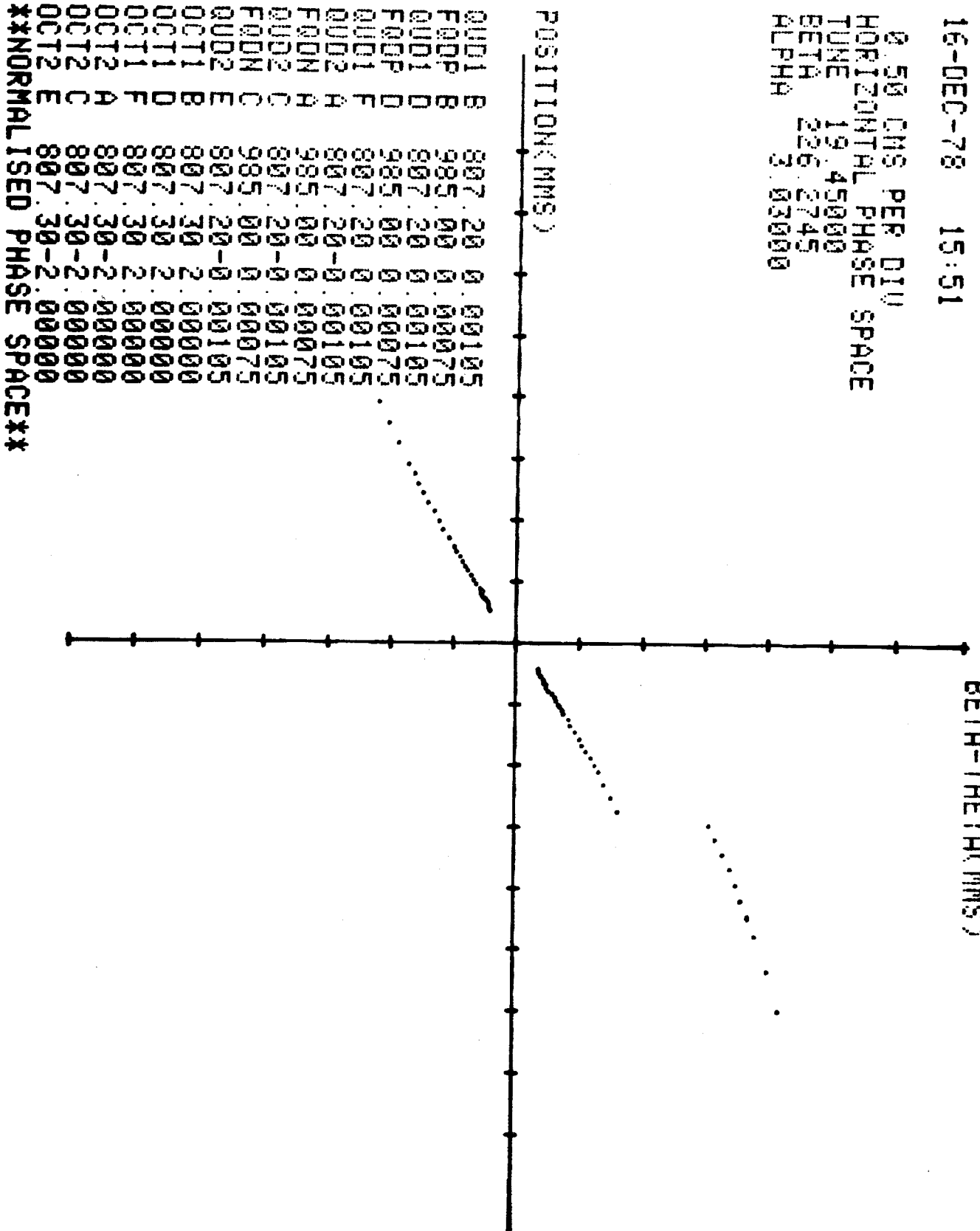
0.50 CMS PER DIV
HORIZONTAL PHASE SPACE
TUNE 19.45000
BETA 226.2791
ALPHA 3.03010



16-DEC-78 15:51

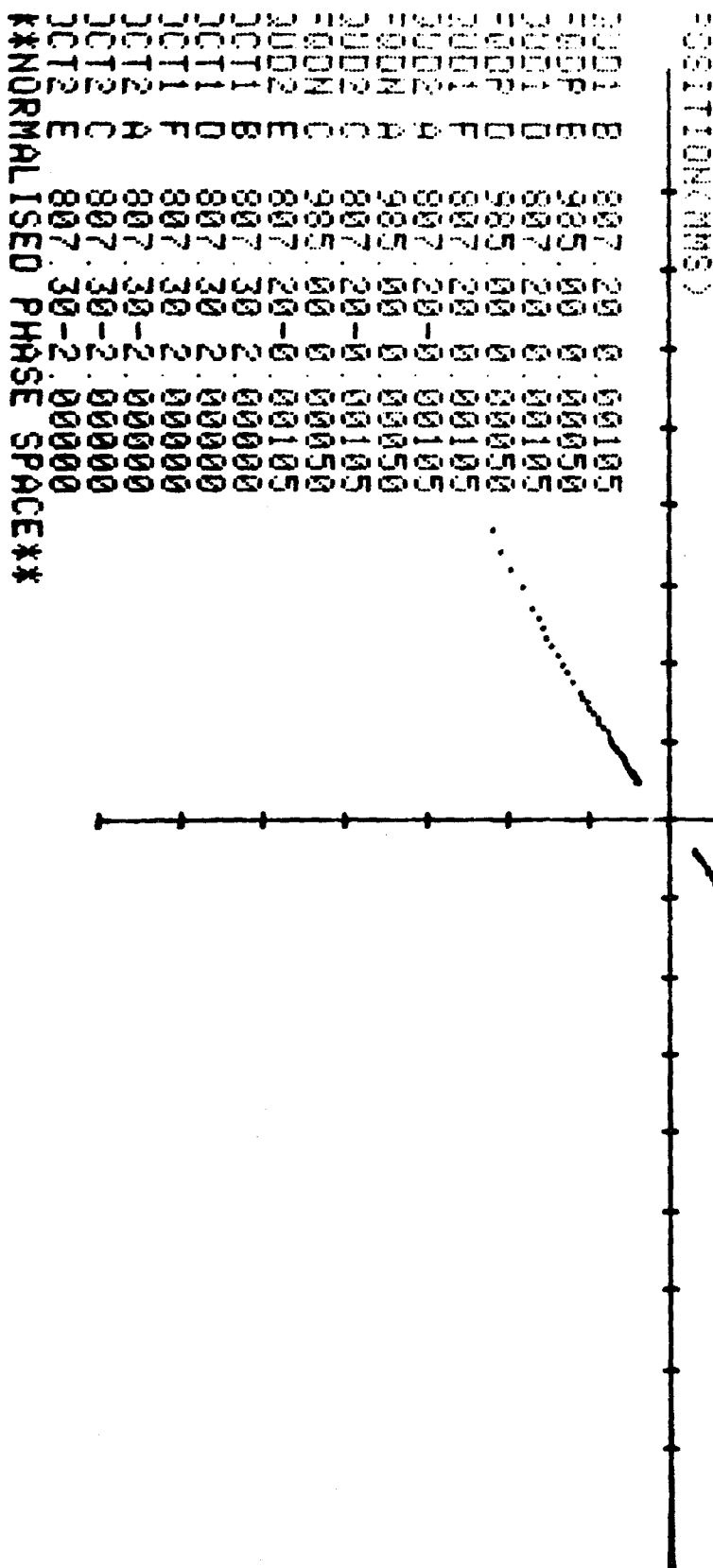
BETH-THETA(MNS)

0.50 CMS PER DIV
HORIZONTAL PHASE SPACE
TUNE 19.45000
BETA 226.2745
ALPHA 3.03600



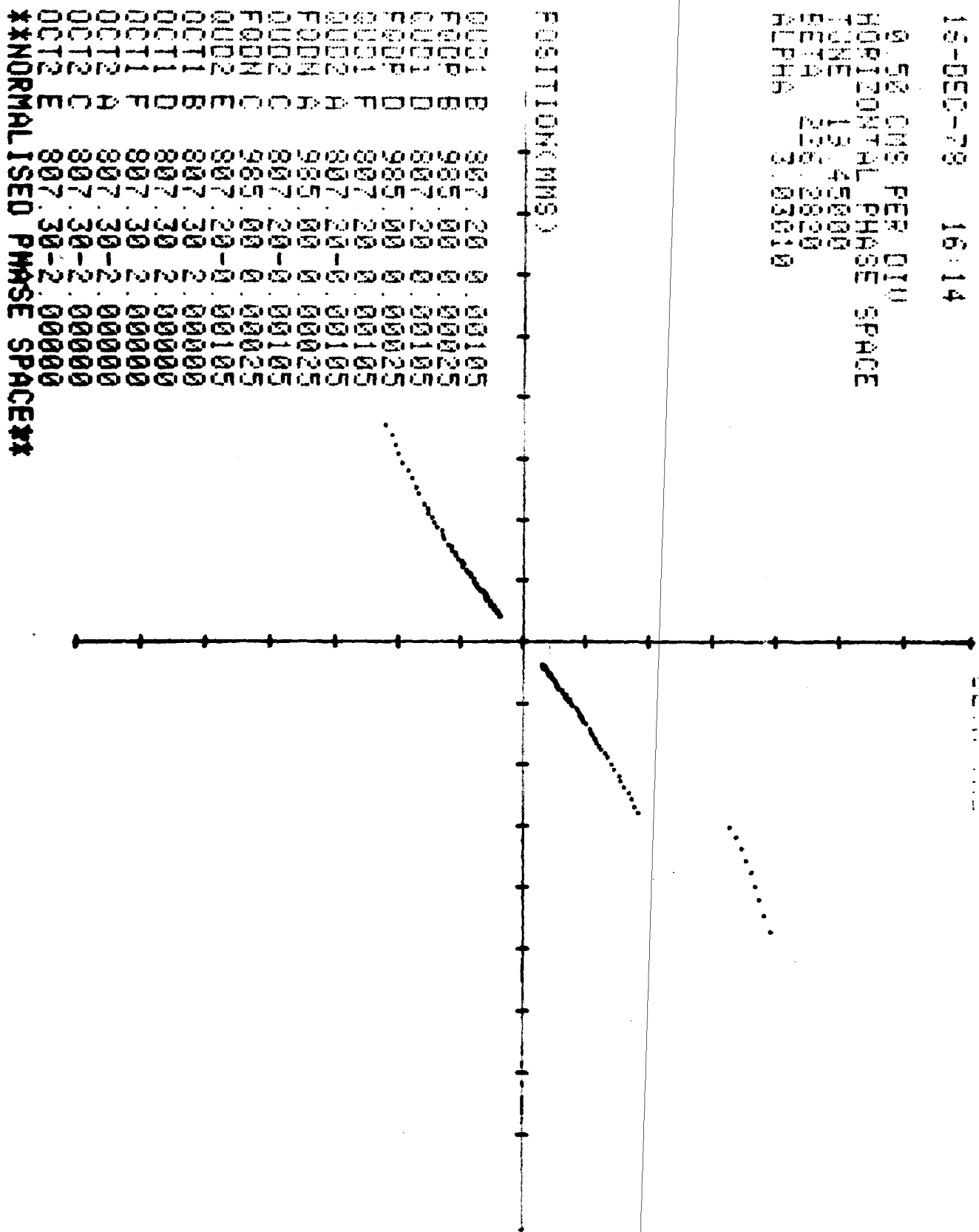
0.56 CMS PER FTU
TOP 1200 NTL PHASE SPACE

1000 900 800 700 600 500 400 300 200 100 0



16-14

PHASE SPACES IN PERIODIC TIME



23-JAN-79 08:58

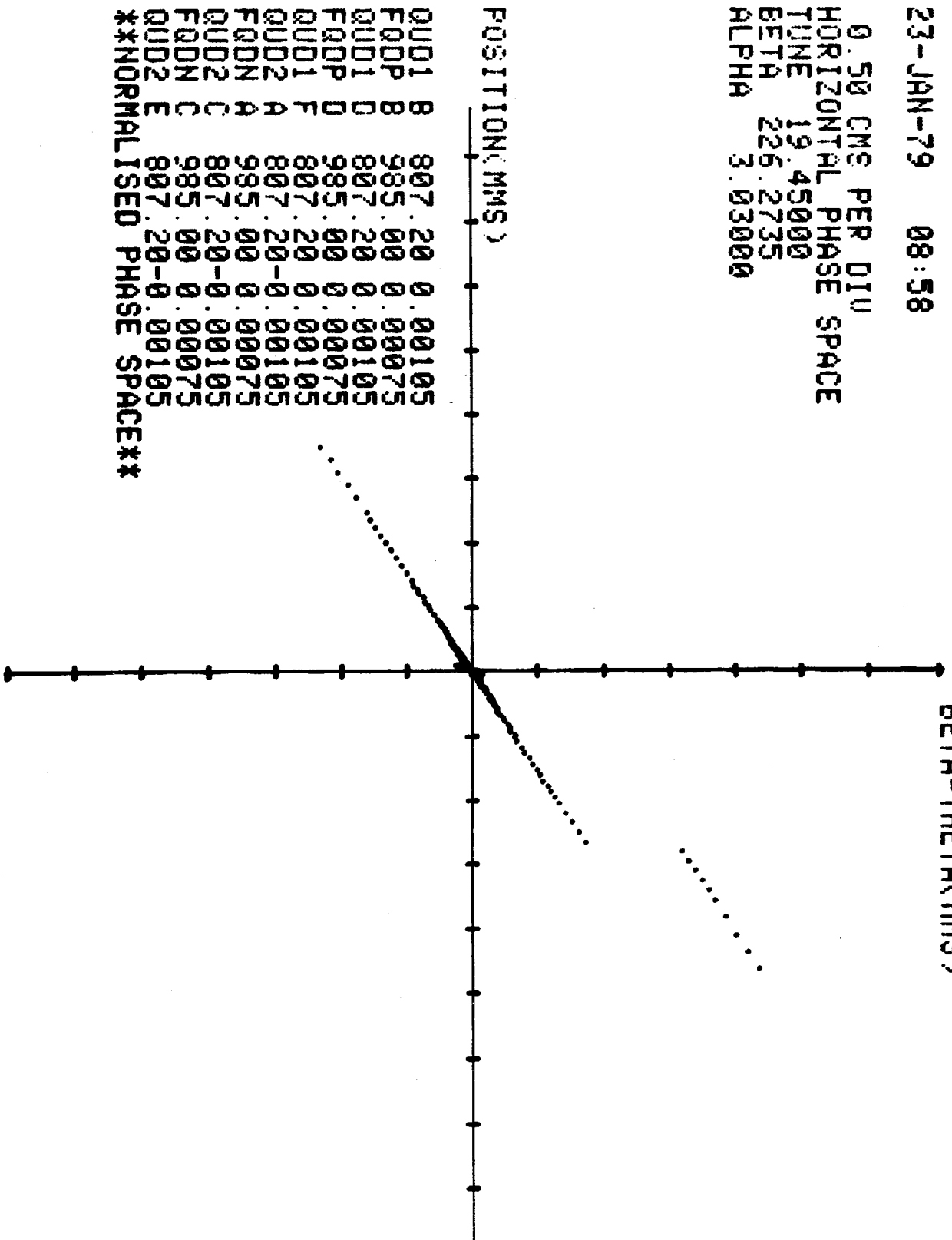
0.50 CMS PER DIV
HORIZONTAL PHASE SPACE
TUNE 19.45000
BETA 226.2735
ALPHA 3.03000

BETA-THETAC(MMS)

POSITION(MMS)

	DUD1	FQDP	QUD1	FQDP	QUD1	FQDN	QUD2	FQDN	QUD2	FQDN	QUD2	E
B	807	.20	985	.60	987	.20	987	.20	987	.20	987	.20
	0	0	0	0	0	0	0	0	0	0	0	0
	0.00105	0.00075	0.00105	0.00075	0.00105	0.00075	0.00105	0.00075	0.00105	0.00075	0.00105	0.00075

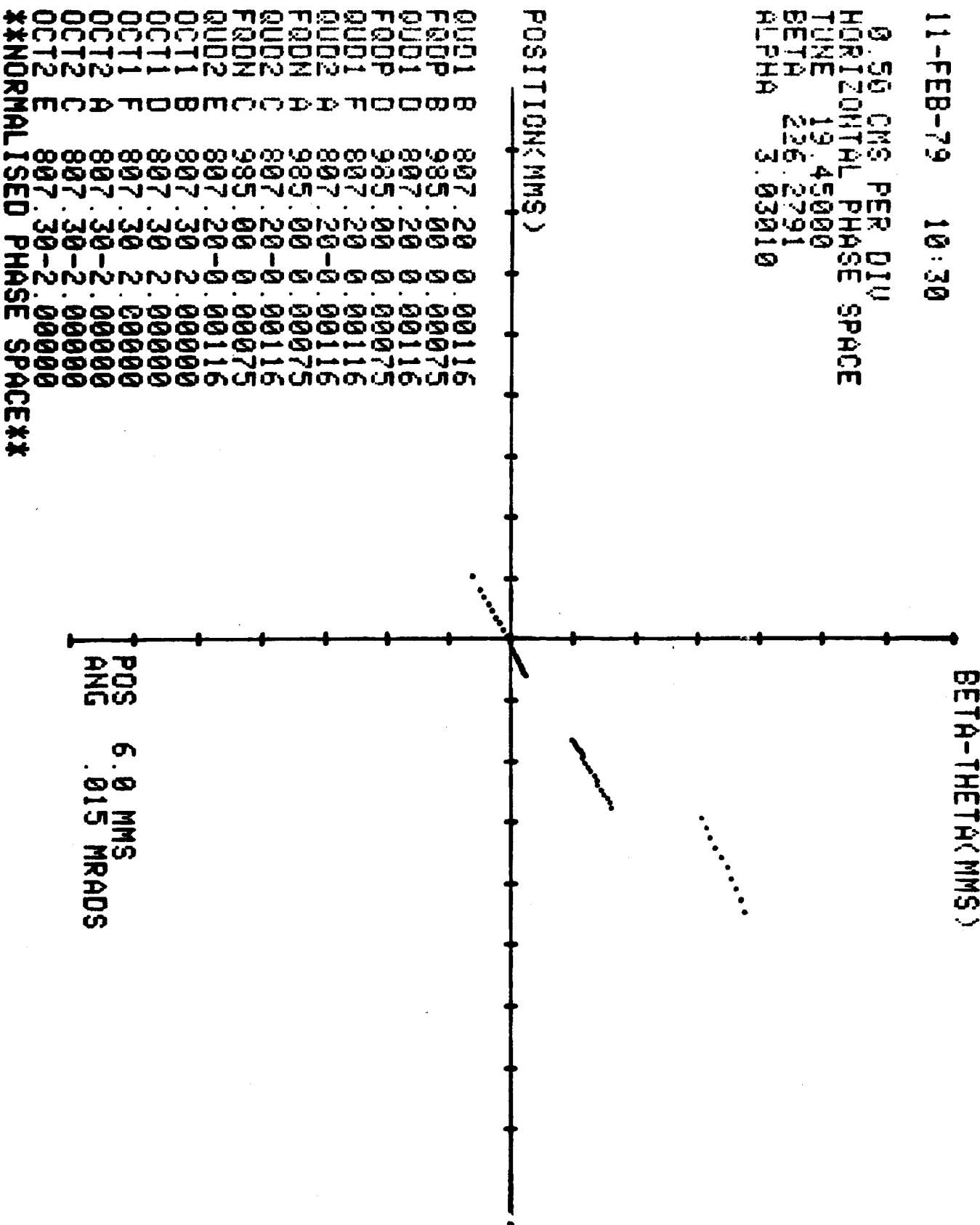
**NORMALISED
PHASE SPACE**



11-FEB-79 10:30

BETA-THETAC(MMS)

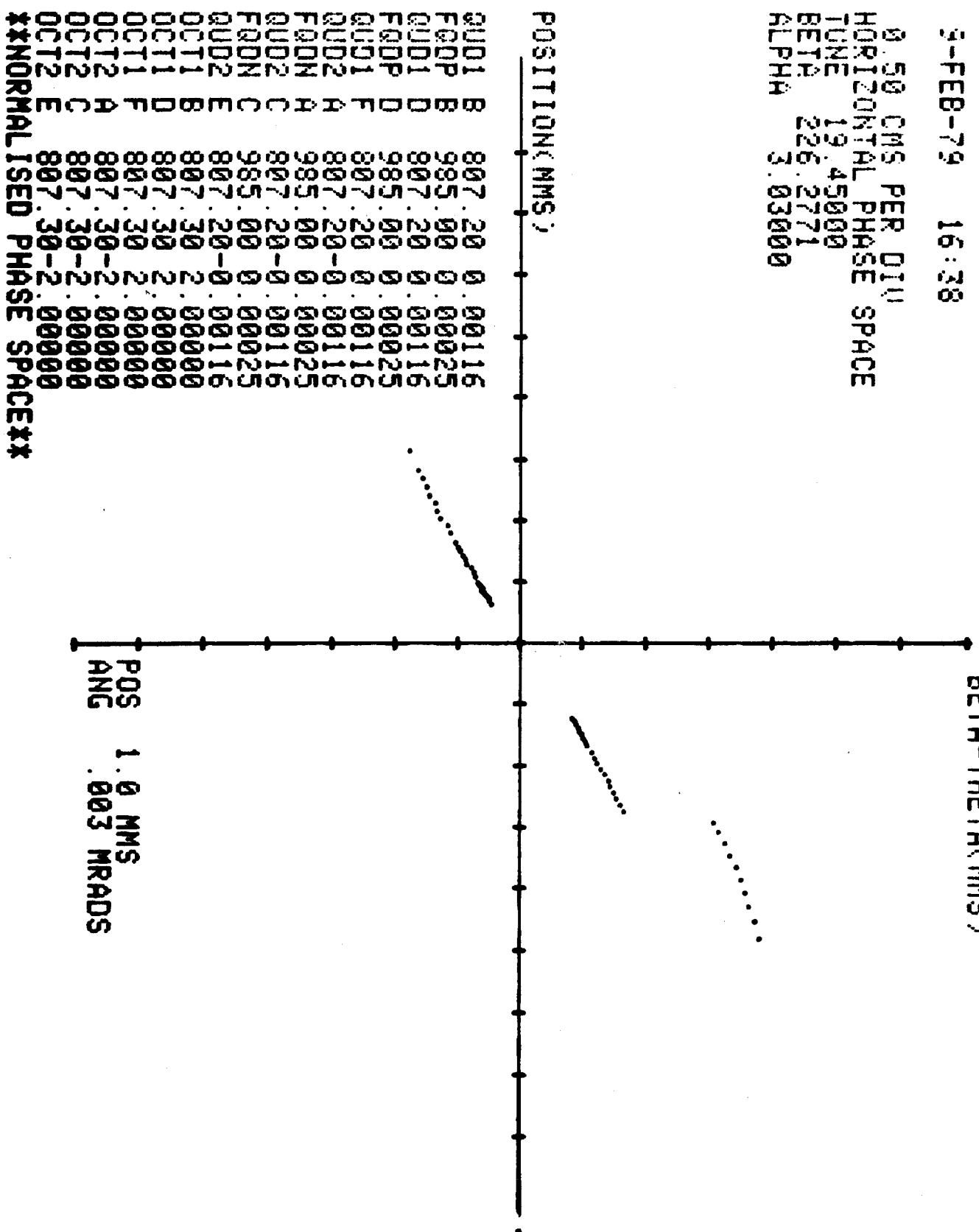
9.55 CMS PER DIV
HORIZONTAL PHASE SPACE
TUNE 19.45000
BETA 226.2791
ALPHA 3.03010



J-FEB-79 16:28

БЕТЫ-ТЕТА (ММС)

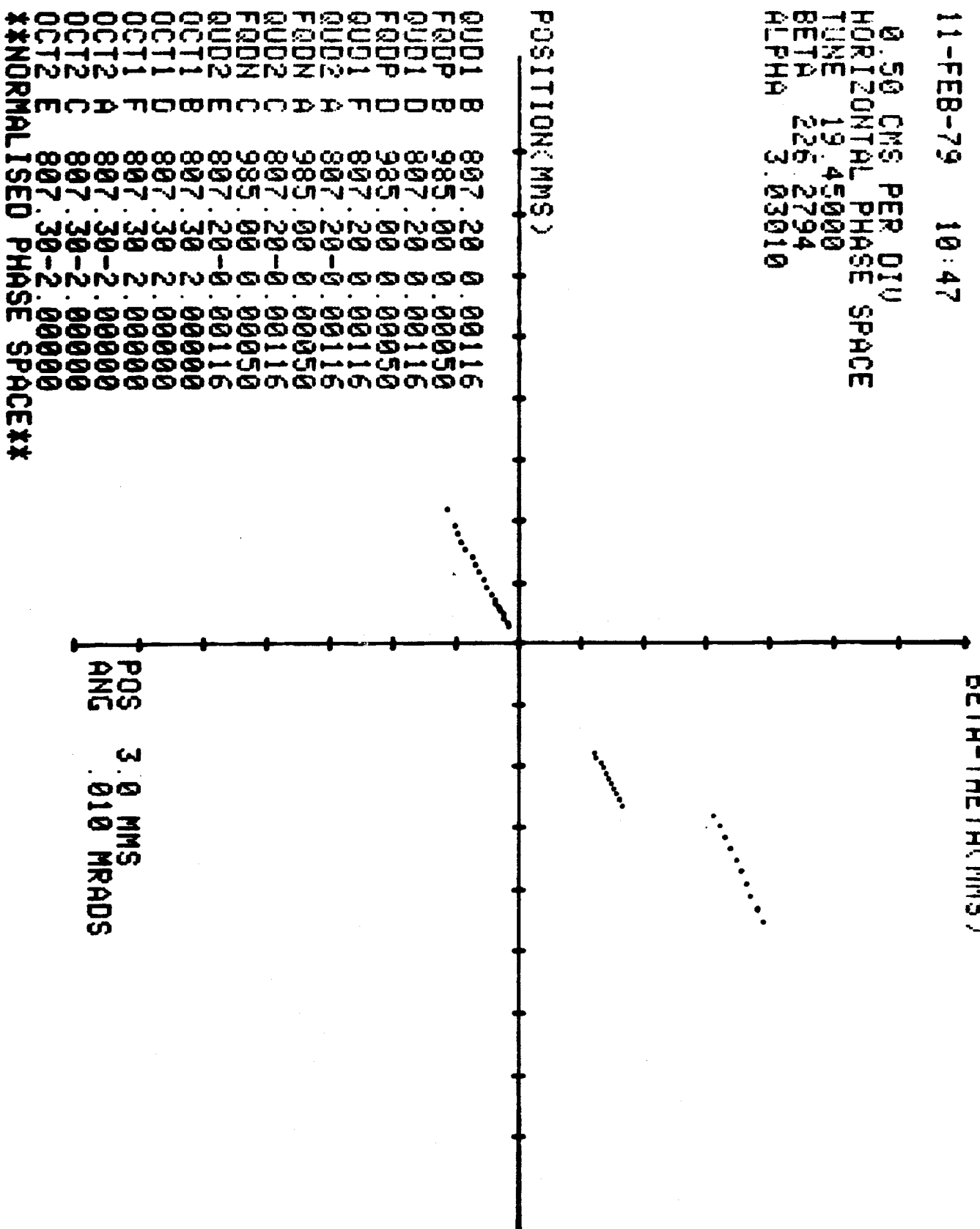
0.50 CMS. PER DIV.
HORIZONTAL PHASE SPACE
TUNE 19.45000
BETA 226.2771
ALPHA 3.03600



11-FEB-79 10:47

BETÀ-THETA(MMS)

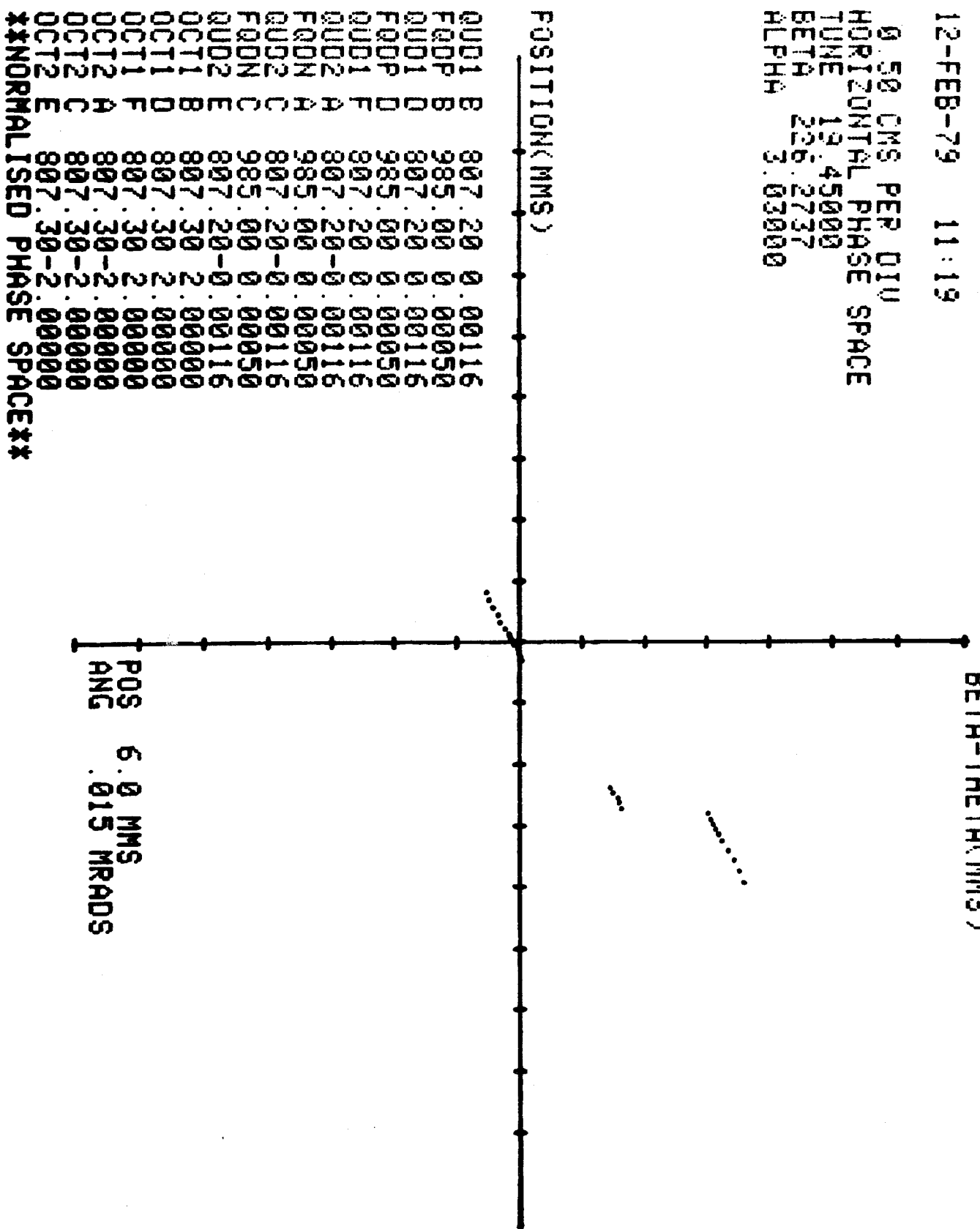
0.50 CMS PER DIV
HORIZONTAL PHASE SPACE
TUNE 19.45000
BETA 22.2794
ALPHA 3.03010



12-FEB-79 11:19

BETÀ-THETA(MMS)

0.50 CMS PER DIV
HORIZONTAL PHASE SPACE
TUNE 19.45000
BETA 226.2737
ALPHA 3.03000

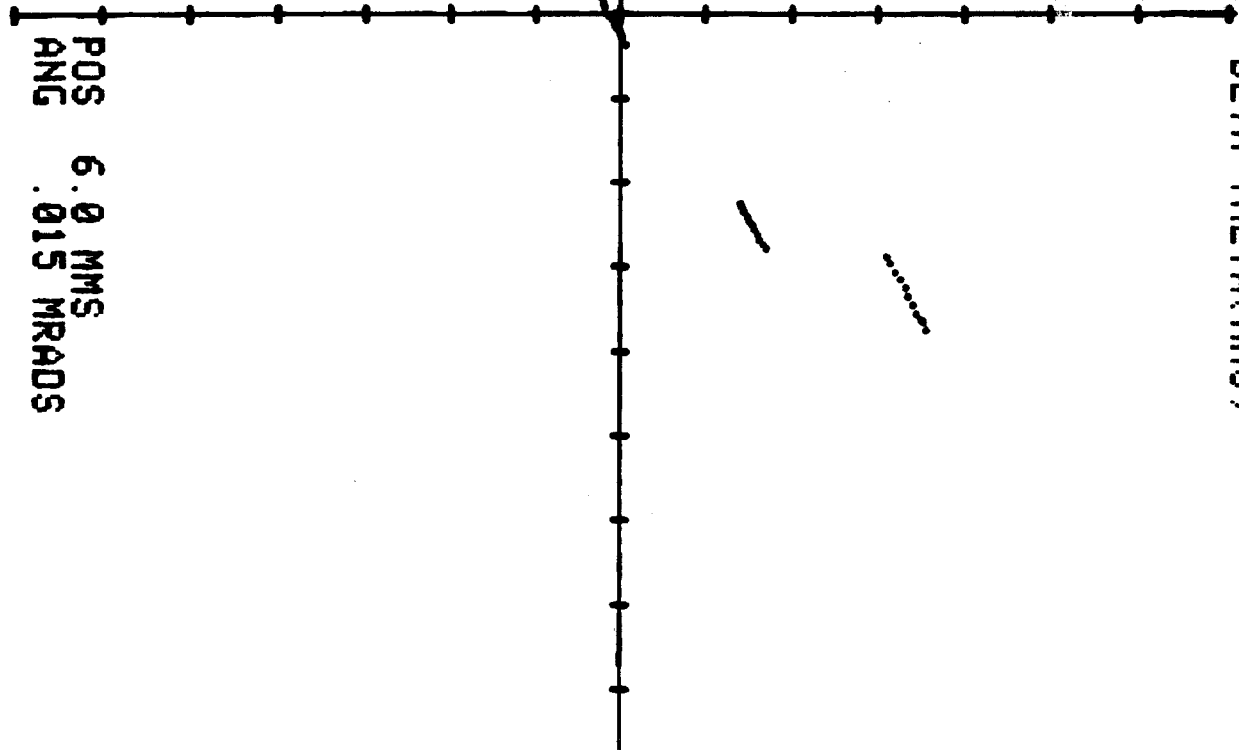


12-FEB-79 09:23

BETA-THETA(MMS)

0.50 CMS PER DIV
HORIZONTAL PHASE SPACE
TUNE 19.45000
BETA 226.2794
ALPHA 3.03010

POSITION(MMS)



QUD1 FQDF 987.20
QUD1 FQDF 985.20
QUD1 FQDF 987.20
QUD1 FQDF 985.20
QUD2 FQDF 987.20
QUD2 FQDF 987.20
QUD2 FQDF 985.20
OCT1 FQDN 985.20
OCT1 FQDN 987.20
OCT1 FQDN 985.20
OCT2 FQDN 985.20
OCT2 FQDN 987.20
OCT2 FQDN 985.20
**NORMALISED
PHASE
SPACE**